Journal of *Nanotheranostics*

MDPI

Review

Intrinsically Selective Nanoplatforms for Precision Therapy and Monitoring

Aurelie F. Brownsberger [1,2,3], Carlie Kudary [2,3,4], Hezekiah H. Williams [1], Shirley Wei [2], Philip Latorre [2], Ryan Eastland [2], Olivia Sayani [2], Jichong Lyu [2], Ryan Davey [2], Victoria Hopkins [2], Ryan K. Roeder [1,3] and Prakash D. Nallathamby [1,2,3,*]

[1] Department of Aerospace and Mechanical Engineering, Bioengineering Graduate Program, University of Notre Dame, Notre Dame, IN 46556, USA; amoutran@nd.edu (A.F.B.); rroeder@nd.edu (R.K.R.)
[2] The Berthiaume Institute for Precision Health, University of Notre Dame, Notre Dame, IN 46556, USA
[3] Harper Cancer Research Institute, University of Notre Dame, Notre Dame, IN 46556, USA
[4] Department of Civil and Environmental Engineering and Earth Sciences, Bioengineering Graduate Program, University of Notre Dame, Notre Dame, IN 46556, USA
* Correspondence: pnallath@nd.edu; Tel.: +1-(574)-631-7868

Abstract

Nanoparticles offer a versatile platform for the selective eradication of pathogenic or diseased cells by integrating therapeutic payload delivery with precision targeting. Precision targeting can be achieved (1) actively through ligand conjugation, (2) passively by exploiting the physiological abnormalities of diseased tissues, or (3) intrinsically through the innate biophysical properties of the nanoparticle. Intrinsically selective nanoplatforms (iNPs) are particularly advantageous when the disease-promoting agent does not possess distinct surface markers, such as in the case of certain "untargetable cancers" or cancers without known targets. Indeed, nanocarriers for chemotherapeutic or gene delivery have achieved selective cancer cell apoptosis without requiring marker presentation, thereby expanding the therapeutic window of the payload. Disease-promoting agents whose physical properties are different from those of healthy cells are also good candidates for intrinsic nanoparticle targeting. For example, antimicrobial nanomaterials have been designed to disrupt bacterial membranes and reduce the risk of antimicrobial resistance by leveraging stiffness differentials between bacterial cell walls and eukaryotic membranes. Nanoparticle systems with intrinsic targeting mechanisms can also enable non-invasive imaging with near-infrared fluorescence, MRI, and photoacoustic imaging for real-time biodistribution tracking and treatment monitoring. This review synthesizes current innovations in nanoplatform design with intrinsic targeting capabilities, spans applications in infectious and non-communicable diseases, and discusses emerging strategies to enhance specificity, overcome resistance, and translate these platforms toward clinical and field deployment.

Keywords: nanotheranostics; intrinsically selective; precision therapy; stimuli-responsive nanoparticles; biomimetic nanoparticles; multimodal imaging; targeted drug delivery; tumor microenvironment; antimicrobial nanomaterials; magnetoelectric nanoparticles

Check for updates

Academic Editors: Dmitri Simberg and Peng Huang

Received: 19 March 2026
Revised: 13 April 2026
Accepted: 29 April 2026
Published: 9 May 2026

Copyright: © 2026 by the authors. Licensee MDPI, Basel, Switzerland. This article is an open access article distributed under the terms and conditions of the Creative Commons Attribution (CC BY) license.

1. Introduction

The promise of nanomaterials for theranostics rests on their ability to concentrate in diseased tissues while sparing healthy organs. Passive targeting has historically relied on the enhanced permeability and retention (EPR) effect, whereby abnormal vasculature

permits nanoparticle extravasation and impaired lymphatic drainage slows clearance. However, EPR is highly heterogeneous across patients, across lesions within the same patient, and even within different regions of a single tumor [1,2]. Mechanistically, leaky vessels alone are insufficient to guarantee delivery: elevated interstitial fluid pressure suppresses convective transport, dense extracellular matrix and stromal remodeling hinder diffusion, and solid stress can compress vessels and further reduce perfusion, collectively restricting deep penetration beyond perivascular regions [1–4]. These physiological barriers help explain why passive accumulation is often modest, inconsistent, and the effect is difficult to generalize beyond cancer.

In contrast, active targeting relies on ligands such as antibodies, peptides, aptamers, or small molecules that are preselected and conjugated to the nanoparticle surface to bind a defined receptor (Figure 1). Although powerful in some settings, this approach introduces its own constraints. Many diseases lack stable surface markers suitable for targeting. Even when markers exist, their expression may be heterogeneous or evolve under therapeutic pressure, and receptor accessibility can be altered by protein-corona formation after systemic administration [5–9]. Targeting strategies that remain effective even when canonical receptor–ligand recognition is unavailable are therefore needed.

In this review, we define intrinsic targeting as selective localization, uptake, retention, or activation that arises from the nanoparticle's innate physicochemical or biophysical properties and their interaction with disease-state biology, rather than from a preselected and conjugated affinity ligand. Intrinsically selective nanoplatforms (iNPs) can therefore exploit host physiology through pathological chemical microenvironments (pH, redox potential, enzymatic activity, oxygen tension), transport barriers, membrane composition, electrical properties, mechanical properties, and metabolic biases. Many iNPs also integrate localized activation by external triggers including light, heat, ultrasound, magnetic fields, and mechanical forces, further sharpening specificity while enabling imaging-guided intervention.

For clarity, we organize intrinsic selectivity into four recurring design strategies: (i) biological interface-driven selectivity, including protein-corona effects, membrane coatings, membrane potential, and metabolic or organelle targeting; (ii) inherent material–tissue affinity; (iii) physicochemical transport biases such as size, shape, and charge; and (iv) mechanical properties such as nanoparticle stiffness (Figure 1). We note that some biomimetic or corona-guided systems lie at the boundary between purely physicochemical and molecularly mediated targeting. We nevertheless include them here when the targeting bias is encoded by the native nano-bio interface—such as membrane composition, topology, or in situ adsorption of endogenous proteins—rather than by an externally grafted targeting ligand [10–13].

This review surveys iNPs across the translational research pipeline. We first summarize representative organic, inorganic, and hybrid platforms and then examine the underlying mechanisms that bias biodistribution and cellular uptake. We next discuss localized activation by biochemical microenvironments and by physical stimuli, including mechanical and rheological cues. Therapeutic applications in cancer, infectious disease, cardiovascular disease, and neurological disorders are then compared alongside their diagnostic and monitoring capabilities. Finally, we outline translational barriers, emerging technologies, and future directions toward personalized nanotheranostics.

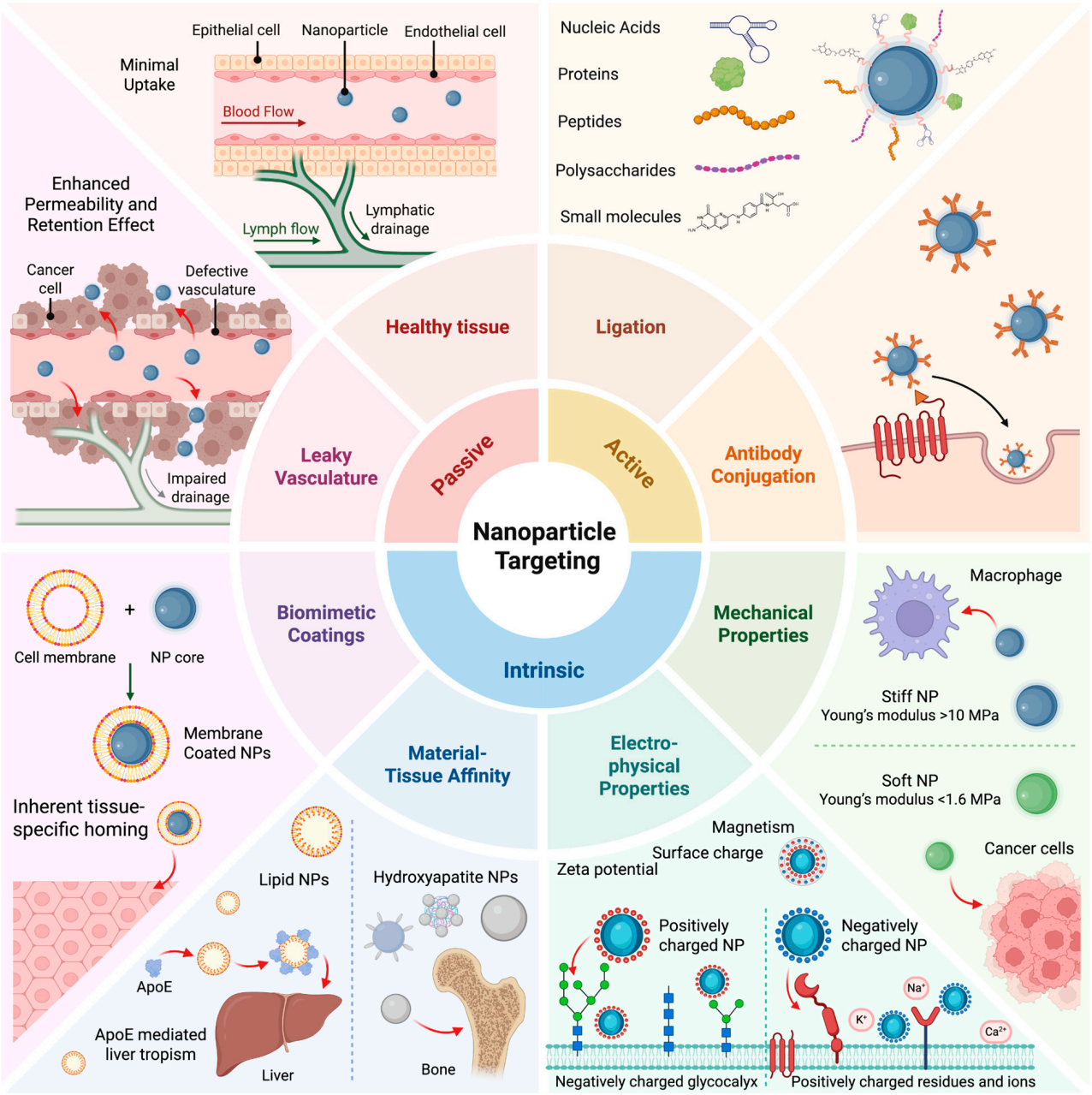

Figure 1. Graphical summary of the three main modes of nanoparticle targeting: passive, active, and intrinsic. Passive targeting primarily relies on the EPR effect in diseased cancerous tissues. Active targeting relies on ligands displayed on the nanoparticle surface. These ligands can be proteins, peptides, nucleic acids, polysaccharides, and small molecules. Antibodies can also be conjugated to NPs for active targeting. Intrinsic targeting can be achieved through several mechanisms, including (i) biomimetic interface-driven selectivity, (ii) inherent material-tissue affinity, (iii) physicochemical transport biases (size, shape, and charge), and (iv) mechanical properties (e.g., nanoparticle stiffness). Created in BioRender. Brownsberger, A. (2026). https://BioRender.com/8owkosy (accessed on 4 March 2026).

2. Material Platforms with Intrinsic Selectivity

A variety of nanoplatforms have been engineered to achieve intrinsic targeting without relying on explicit receptor–ligand interactions. This section highlights representative examples across inorganic and organic materials, summarized in Table 1. Generalizable mechanisms for intrinsic targeting will be reviewed in Section 3.

2.1. Inorganic Nanoplatforms

Inorganic nanoparticles possess unique physicochemical properties that can be leveraged to enable intrinsic targeting. In addition, many inorganic platforms exhibit robust heat and light stability, imaging contrast for detection, tunable optical properties, and environmental adaptability, making them multivalent agents for targeted delivery and therapeutic effects. Across inorganic iNPs, intrinsic selectivity is most often enabled through (i) size/shape-dependent transport, (ii) environment-adaptive surface chemistry (e.g., pH- or redox-dependent behavior), and (iii) field-responsive guidance or heating. Several examples below illustrate each of these strategies.

Cerium oxide nanoparticles, also known as nanoceria, may target specific cellular environments based on their redox state by switching between antioxidant and pro-oxidant states (Ce^{3+}/Ce^{4+}) on the surface of the nanoparticle. These states depend on the pH and oxidative stress levels of the destination microenvironment. Therefore, these nanoparticles extend beyond EPR by targeting the pathophysiological state of the target cell instead of relying on leaky vessels [14,15]. Moreover, nanoceria can intrinsically switch chemical behavior based on the local environment, allowing for "smart" targeting and activation [16–18]. As such, it acts as a protective antioxidant in neutral pH typical of healthy cells, and as a cytotoxic "kamikaze" in acidic microenvironments typical of cancer cells [19].

Calcium phosphate (CaP) bioceramic systems have long been used for cell targeting and gene transfections in vitro. CaP nanoparticles have been proposed to intrinsically enter cells through endocytosis facilitated by interactions between the positively charged calcium ions and negatively charged caveolae, which are specialized microdomains on the plasma membrane [20]. Literally meaning "little caves", caveolae are dynamic endocytic carriers and form endocytic vesicles of 50 to 60 nm in a clathrin-independent manner [21]. CaP nanoparticles have been demonstrated to efficiently deliver exogenous cargo (e.g., nucleic acids and proteins) to stem cells and primary neural cells while maintaining low cytotoxicity [22]. These properties make CaP nanoparticles a promising platform for achieving cellular uptake without the need for additional surface modifications or targeting ligands.

Hydroxyapatite (HA), is a specific CaP with composition ($Ca_{10}(PO_4)_6(OH)_2$), similar to bone mineral. HA exhibits a natural affinity for bone tissue and can be used to intrinsically target bone matrix. Beyond its bone affinity, HA is highly biocompatible and osteoconductive, rendering it an attractive material for orthopedic cases [23–26]. HA nanoparticles (nHA) have exhibited higher uptake in bone than surrounding tissues when systemically administered in animal studies [27]. However, macrophage uptake of nHA particles resulting in high liver and spleen accumulation was also observed. As such, localized administration or implantation of nHA particles may be ideal to intrinsically target bone and bypass macrophage clearance. Combinations of HA with bisphosphonates have also been explored to further enhance bone binding through calcium chelation [28–30]. In osteoporosis animal models, HA-based nanoconjugates of mPEG, PLGA, and risedronate (a bisphosphonate) were found to increase the relative bioavailability of risedronate 6-fold and 4-fold after intravenous and oral administration of nanoparticles, respectively, over commercially available risedronate tablets and showed significant enhancements in bone micro-architecture [31,32]. Bone-homing hydroxyapatite nanoparticles can also serve as theranostic platforms by radiolabeling with technetium-99m [27,33], phosphorus-32 [34], or rare-earth metals such as lutetium-177 [35].

Semiconductor nanocrystals, widely known as quantum dots, can also be engineered to exhibit intrinsic targeting capabilities. For example, charge-reversal zinc oxide (ZnO) quantum dots coated with charge-reversal polymers switch from negatively charged surfaces at physiological pH to positively charged surfaces at the slightly acidic extracellular pH of tumors, allowing selective adhesion to tumor cell membranes [36,37]. Sulfonic acid-functionalized graphene quantum dots (sulfonic-GQDs) also achieve tumor cell nuclear targeting without bioligand modification by exploiting the high interstitial fluid pressure (IFP) of solid tumors [38]. Under high-IFP conditions, pressure-enhanced membrane deformation appears to facilitate transient defects through which the otherwise membrane-repelled, negatively charged sulfonic-GQDs can traverse cancer cell membranes. The particles subsequently accumulate in nuclei both in vitro and in vivo; molecular dynamics simulations reproduced this behavior and supported a pressure-assisted transport mechanism (Figure 2) [38]. These examples show promise for theranostic applications because quantum dots are bright and stable light emitters due to intraparticle quantum confinement and are substantially less susceptible to photobleaching than organic fluorescent dyes, making them suited to traceable drug delivery, multicolor bioimaging, and real-time monitoring of targeted payloads [39–41].

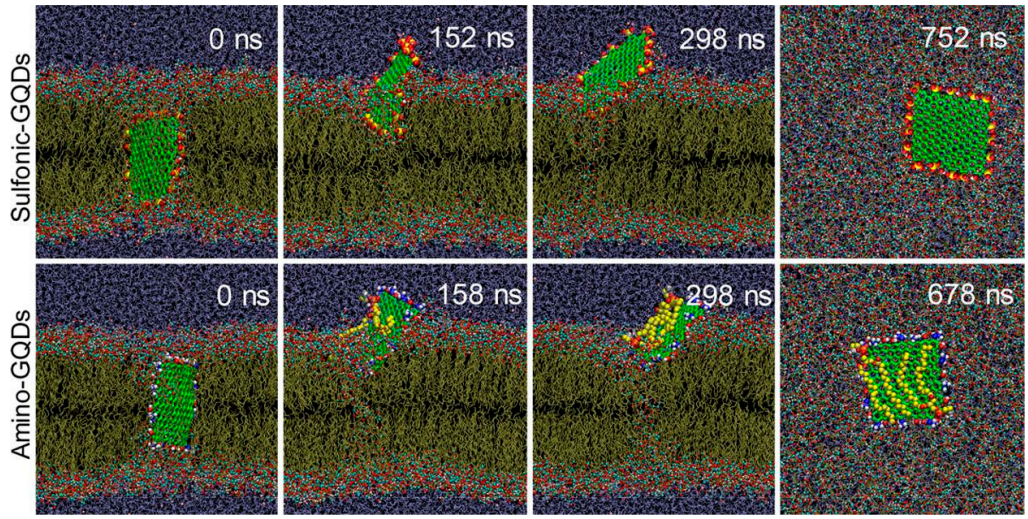

Figure 2. Functionalized graphene quantum dots crossing through cell membranes in high interstitial fluid pressure conditions. Representative trajectories of the molecular dynamics (MD) simulations with sulfonic-GQDs and amino-GQDs detached from the lipid membranes. The amphiphilic GQDs were composed of a hydrophobic graphene core (2.21 × 2.41 nm^2) and a hydrophilic periphery functionalized with SO_3^- or NH_{3+}. The cell membrane is modeled as a negatively charged phospholipid bilayer for simplification. Water is shown in violet, the GQDs are shown as large spheres (carbon, green; sulfur, yellow; oxygen, red; nitrogen, blue; hydrogen, white) and the phospholipids are shown as tan lines with the hydrophilic charged atoms as small colored spheres (hydrogen, white; oxygen, red; nitrogen, dark blue; carbon, cyan; phosphorus, orange). Reprinted with permission from Ref. [38], 2017, American Chemical Society.

Magnetic nanoparticles (MNPs), typically smaller than 25 nm, utilize superparamagnetism to exhibit zero net magnetization in the absence of an external magnetic field, but show strong magnetization once a magnetic field is applied [42]. MNPs can be physically guided or retained at a specific site by a magnetic field gradient. Examples are iron oxide nanoparticles such as magnetite (Fe_3O_4) or maghemite (γ-Fe_2O_3) [43,44]; carbide nanoparticles like cobalt carbide (Co_2C) and iron carbide (Fe_3C) [45,46]; and tantalum carbide (Ta_4C_3) [47]. Some MNPs have a biomimetic interface, drawing inspiration from ferritin proteins [48–50] and bacterial magnetosomes [51–53]. Magnetic targeting has been shown to concentrate drug-loaded particles in tumors or other or-

gans, independent of tissue architecture, such as vascular pore size and blood vessel density [54–56]. Beyond drug delivery, MNPs can be used as MRI contrast agents and for localized hyperthermic treatments [57–59].

Inorganic nanoplatforms frequently couple intrinsic selectivity with stable core-dependent multifunctional properties (e.g., optical, magnetic, redox). Organic and polymeric nanoplatforms offer modular chemistry for tuning charge, degradability, and stimulus responsiveness while maintaining biocompatibility.

2.2. Organic and Polymeric Nanoplatforms

Organic nanoplatforms—made from proteins, carbohydrates, lipids, and polymers—are often favored for their superior biocompatibility, biodegradability, and low toxicity relative to many inorganic materials [60,61]. These include liposomes, polymeric nanoparticles, micelles, dendrimers, among others. These platforms are often intrinsically selective because their surface charge, surface chemistry, hydrophobicity, and deformability can be tuned without appending a classical targeting ligand [31,62]. Ligand-free selectivity can therefore be engineered into diverse organic materials, as described below.

Among organic nanoparticles, lipid nanoparticles (LNPs) have demonstrated a strong capacity to encapsulate genetic materials and protect them from enzymatic degradation [63]. Their success has been exemplified by recent clinical applications, including mRNA vaccines for COVID-19 and emerging cancer immunotherapies [64,65]. Beyond cargo protection, LNPs exhibit organ- and cell-level selectivity that is strongly governed by composition [10–13,66–70]. Many canonical intravenous LNP formulations display liver tropism after rapid adsorption of ApoE and other serum proteins, which bridge the particles to LDL receptor family pathways on hepatocytes [10,12,13]. Importantly, this targeting emerges from endogenous corona formation rather than a preselected and conjugated exogenous ligand, which supports classification as an interface-mediated form of intrinsic selectivity where molecular uptake pathways are recruited during circulation. At the cellular level, ionizable lipids become protonated in acidifying endosomes and promote membrane destabilization, non-bilayer intermediates, and endosomal escape, thereby enabling cytosolic release of encapsulated nucleic acids [66,67]. PEG-functionalized lipids further shape biodistribution by modulating particle size, aggregation, circulation time, and the kinetics of corona remodeling [68,69].

More broadly, LNP biodistribution and intracellular performance are tightly linked to molecular-scale structure–property relationships. Headgroup chemistry and apparent pKa determine when ionizable lipids acquire charge; tail saturation, branching, and cholesterol content regulate bilayer order or disorder, lateral packing defects, bending rigidity, and compressibility; and PEG-lipid chain length plus desorption kinetics influence colloidal stability, corona remodeling, and cell access [12,67–70]. More disordered and compressible interfacial regions can facilitate membrane fusion and endosomal escape, whereas highly ordered shells may improve circulation stability but reduce deformation and cellular wrapping. Intrinsic selectivity in lipidic systems should therefore be viewed as a tunable consequence of composition, not simply of particle identity.

Polymeric nanoparticles are a widely used type of organic nanoparticles that primarily exhibit intrinsic targeting at the cellular level through physicochemical interactions that bias endocytic uptake mechanisms. Polymeric nanoparticles can exhibit selective internalization across tissues without the need for explicit receptor–ligand recognition because different cell types preferentially exhibit distinct uptake routes [71–73]. Cellular internalization of polymeric nanocarriers is thus governed by particle size, surface charge, rigidity, and chemical composition, which collectively determine the endocytic pathways engaged [74–76].

Polymeric nanoparticles may also be internalized through pinocytosis or phagocytosis, particularly in immune and phagocytic cell populations [77]. Following uptake, polymeric nanoparticles such as those with integrated acid-sensitive bonds, light-sensitive agents, enzyme-sensitive linkers, or other environment-responsive moieties, can further achieve functional selectivity through stimulus-responsive drug release [71,78–80]. This process can be triggered by intracellular and extracellular cues such as pH, temperature, and redox reactions [80,81]. These uptake and release characteristics enable polymeric nanoparticles to preferentially deliver therapeutic or diagnostic cargo to diverse cellular and tissue environments.

Table 1. Representative intrinsically selective nanoplatforms discussed in this review, including selectivity mechanism, targets, and theranostic applications.

Platform Class	Representative Example(s)	Selectivity Mechanism	Target(s)	Theranostic Applications	References
Inorganic redox NPs	Nanoceria (CeO_2)	Environment-dependent Ce^{3+}/Ce^{4+} switching in acidic or oxidative niches	Tumors and oxidative or inflamed tissues	Redox modulation plus imaging-enabled therapy	[14–19]
Mineral-affinity ceramics	CaP, hydroxyapatite	Caveolae interaction and natural bone-mineral affinity	Stem cells, bone matrix, skeletal lesions	Gene delivery and radionuclide theranostics	[20–35]
Quantum dots (QDs)	ZnO QDs, sulfonic-graphene QDs	Charge-reversal or IFP-assisted membrane translocation	Solid tumors and, in some cases, tumor nuclei	Fluorescence tracking and image-guided delivery	[36–41]
Magnetic nanomaterials	Fe_3O_4, ferrites, Magnetostrictive core piezoelectric silica shell	Field-guided retention, magnetothermal activation	Tumors or selected organs independent of pore size	MRI and magnetic hyperthermia	[42–59,82,83]
Lipid nanoparticles	mRNA-LNPs with ionizable lipids	ApoE/corona-guided liver uptake; endosomal pH response	Hepatocytes, endosomes, extrahepatic tissues after reformulation	Nucleic-acid delivery with trackable biodistribution	[10,12,13,66–70]
Polymeric nanoparticles	Micelles, dendrimers, stimulus-responsive polymers	Size, charge, rigidity, and chemistry-biased endocytosis	Cell-type-dependent uptake routes	Programmable drug or gene release	[71–81]
Biomimetic membrane-coated NPs	RBC, platelet, immune-cell, cancer cell coatings	Native membrane composition, protein topology, emergent corona	Inflamed endothelium, pathogens, homotypic tumors, immune niches	Stealth plus multimodal therapy or imaging	[11,84–94]
Organelle/metabolic platforms	DLC-based carriers, glycopolymers	Membrane potential and metabolic avidity	Mitochondria, endosomes, glycolytic tumors	Metabolic therapy and intracellular imaging	[62,95–104]
Mechanically tuned carriers	Lipogels, hydrogel core–lipid shell NPs	Tunable stiffness and deformability	Cancer cells versus macrophages, depending on modulus	Selective delivery or immune reprogramming	[105–108]

Abbreviations: ApoE, apolipoprotein E; CaP, calcium phosphate; DLC, delocalized lipophilic cations; GQDs, graphene quantum dots; HA, hydroxyapatite; IFP, interstitial fluid pressure; LNPs, lipid nanoparticles; MRI, magnetic resonance imaging; mRNA, messenger RNA; NPs, nanoparticles; PLGA, poly(lactic-co-glycolic acid); QDs, quantum dots; RBC, red blood cells; ZnO, zinc oxide.

3. Mechanisms of Tissue-Specific Intrinsic Selectivity

In this section, we will conceptualize the previous nanoplatform examples into generalizable mechanism-property relationships that bias biodistribution and cellular uptake independent of receptor–ligand recognition.

3.1. Surface Charge and Zeta Potential

The zeta potential of nanoparticles is a quantification of the electrostatic attraction or repulsion between particles. The zeta potential can be fine-tuned to improve the stability of nanoparticles, and can also be leveraged to target specific tissues or cell types. For instance, mucus-rich tissues (e.g., lungs) composed of glycoproteins with anionic substructures, such as sulfonic acid and sialic acid, strongly attract positively charged nanoparticles but allow neutral and negatively charged particles to pass through. The surface charge of a nanoparticle should therefore be designed with the route of administration in mind. For example, buccal and pulmonary mucous membranes are likely to trap positively charged nanoparticles that are inhaled. Conversely, noncationic nanoparticles $\leq$34 nm in size have been shown to rapidly translocate from the lung to the mediastinal lymph nodes following inhalation [109]. In the same study, cationic nanoparticles 6 nm in size were shown to pass through the alveolar-capillary membrane and enter the bloodstream.

The zeta potential of a nanoparticle is not necessarily a static parameter. In recent years, several groups have developed nanoparticles capable of changing the zeta potential upon a physical or chemical stimulus such as pH [110–113]. In addition to playing an important role in tissue-targeting, a change in zeta potential can also be tuned to allow for on-demand cellular uptake. Piezoelectric nanoparticles were designed to undergo charge polarization and thus a change in zeta potential upon the application of a magnetic field [82]. This magneto-electric effect resulted in a decrease in zeta potential from -6.8 mV to -11.2 mV upon the application of a 30 Gauss magnetic field, which led to increased permeation in a panel of cancer cells [82,83].

3.2. Biomimetic Membrane-Coated Nanoparticles

Membrane-coated nanoparticles first emerged in 2011 when poly (lactic-co-glycolic acid) (PLGA) nanoparticles were co-extruded with erythrocyte membranes [73]. Biomimetic coatings have since gained traction in nanomedicine, with exploration of many types of membranes, including red blood cells, stem cells, cancer cells, and leukocytes, to name a few [11,84–86]. Several strategies can be leveraged to fuse a biological membrane to a core nanoparticle, including extrusion, microfluidic electroporation, flash nanocomplexation, and sonication [84,87]. The nanoparticle core can be organic or inorganic, depending on the desired physical, chemical, and biological properties (Figure 3). Thus far, PLGA cores have remained most commonly investigated due to their high drug loading capacity, tunability of degradation mechanism, and biocompatibility [84]. Inorganic cores such as mesoporous silica and gold have also been explored as opportunities to access multifunctional theranostic capabilities, including drug delivery, radiolabeling, and photothermal therapy [88,89].

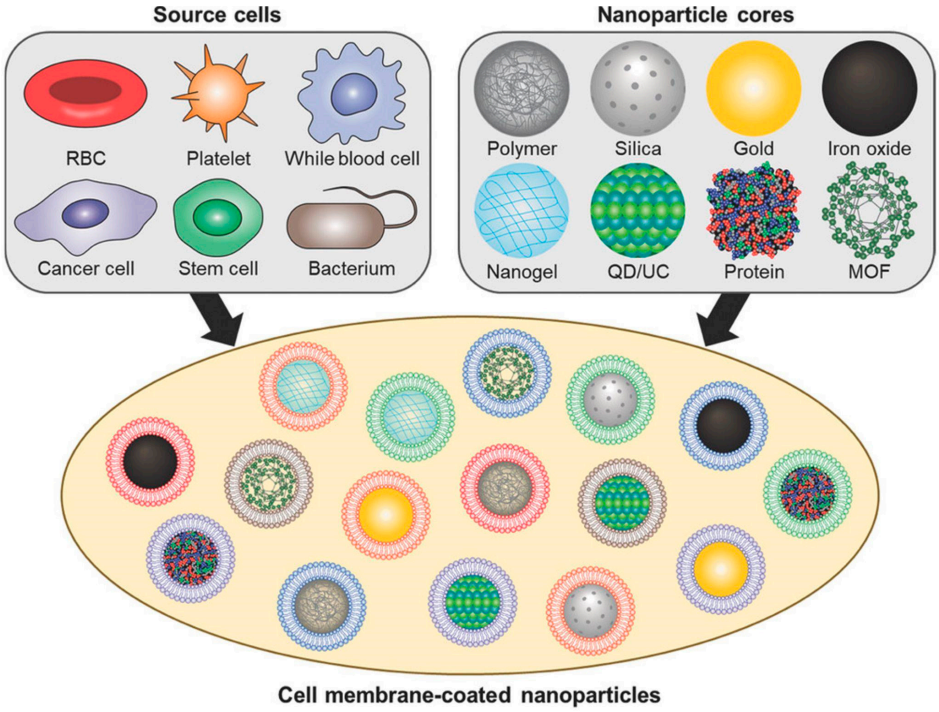

Figure 3. Cell membrane-coated nanoparticles. A variety of cell types have been used as sources of membranes to coat nanoparticles. Distinct cell membrane types provide unique properties and functionality to nanoparticulate cores. Nanoparticle cores can be selected depending on the desired application. Reprinted with permission from Ref. [11], 2018, John Wiley and Sons.

Biomimetic membrane-coated nanoparticles frequently exhibit long circulation times, stealth properties, and tissue-biased interactions, but their classification requires nuance. Their surface identity is not static: native membrane proteins and glycans can mediate homotypic adhesion or immune recognition, while serum-derived coronas can recruit ApoE and other opsonins that redirect uptake toward hepatic or mononuclear phagocyte pathways [10–13,84–87]. Lipid composition and membrane mechanics—including cholesterol content, bilayer disorder, compressibility, and lateral protein organization—govern deformability, immune evasion, and cellular wrapping. Consequently, membrane-coated systems may be classified as intrinsically selective when the targeting bias arises from endogenous membrane composition or emergent corona formation rather than from preselected and conjugated exogenous affinity ligands. Within this framework, immune-cell-coated nanoparticles can recognize inflammatory or abnormal antigenic surfaces [86], platelet membrane-coated nanoparticles can engage pathogens or damaged endothelium [90], cancer cell membrane coatings promote homotypic accumulation in tumors [87,91–93], and mesenchymal stem cell membranes preserve the tissue tropism linked to their source cells [94]. As an illustration of this principle, PLGA-core nanoparticles coated with adipose-derived mesenchymal stem cell (ADSC) membranes retained the original homing properties of ADSC. When administered to rheumatoid arthritis murine models, the nanoparticles localized to the animals' inflamed joints and improved the local delivery of anti-inflammatory agents [94].

3.3. Cell Metabolism-Targeted Platforms

Mitochondria are the intracellular production centers of adenosine triphosphate (ATP) and are also responsible for several other processes essential to cell function and fate. As such, mitochondria are an important therapeutic target in many diseases, such as neurodegeneration, metabolic disorders, ischemia, and cancers [62,95]. These

subcellular organelles have a double-membrane system with a highly negative membrane potential around −180 to −200 mV [96]. Delocalized lipophilic cations (DLCs), such as mitoquinone mesylate, rhodamine 123, dequalinium, and JC-1, can be utilized to leverage the negative membrane potential of mitochondria [96,97]. Several studies have employed DLC-nanotechnologies (such as micelles, self-assembling vesicles, and DLC-conjugated anionic polymeric nanoparticles) for rapid and efficient mitochondrial targeting [62,98,99]. Beyond mitochondrial targeting, DLC-conjugated cationic and charge-neutral polymers were both shown to accumulate in endosomal vesicles [62]. DLC-based nanoparticles may therefore be a suitable approach to intrinsically target the mitochondria or the endosome based on the nanoparticulate construct.

Cellular glucose metabolism is upregulated in certain diseased states and can also be targeted. One of the most notable examples is the Warburg effect, in which cancer cells shift to aerobic glycolysis. This prioritizes lactate formation over mitochondrial oxidative phosphorylation, requiring the cells to increase their glucose uptake to keep up with their metabolic demands [100,101]. A strategy to target this diseased cellular glucose metabolism is to use glucose moieties in the core composition of nanoparticles. For example, glucose single-chain polymer nanoparticles were developed to target tumors using the endocytic pathway [102]. At ~10 nm in size, these glycopolymeric nanoparticles were demonstrated to be capable of drug encapsulation and release [103]. Beyond oncological applications, glycopolymeric nanoparticles synthesized with mannose or galactose have also exhibited molecular recognition with surface-immobilized proteins, such as *E. coli* heat-labile toxin. Upon motif recognition, these small polymeric nanoparticles undergo intermolecular crosslinking to form a film, wrapping the surfaces displaying the molecular recognition motifs [104].

3.4. Cell Stiffness Differentials

The mechanical properties of nanoparticles can also be engineered to exploit differences in stiffness between cell types or between healthy and diseased cells. Nanoparticle stiffness can be precisely tuned via crosslink density, hydration level, shell thickness, lipid composition, and core–shell architecture, generating carriers that span highly deformable nanogels to rigid polymeric assemblies [105–108]. Softer particles (Young's modulus < 1.6 MPa, as measured by atomic force microscopy) have been shown to preferentially accumulate in cancer cells [105], likely because they deform more readily, traverse constricted biological spaces, evade certain phagocytic checkpoints, and exhibit enhanced tumor accumulation. In contrast, stiffer particles (Young's modulus >10 MPa) promote stronger membrane wrapping, greater mechanotransduction, and more efficient uptake by macrophages and other phagocytes [105–108]. For example, rigid nanoparticles composed of the amphiphilic copolymer PLA-b-PItEG deformed tumor-associated macrophage (TAM) membranes, activated mechanosensitive potassium channels, and triggered downstream signaling that reprogrammed these pro-tumorigenic TAMs toward antitumor phenotypes (Figure 4) [108]. Optimal nanoparticle stiffness is thus highly context-dependent, varying with particle size, shape, surface chemistry, protein corona composition, and the local mechanical microenvironment. Overall, nanoparticle mechanical properties are best viewed as a tunable continuum rather than a simple binary classification of "soft" versus "rigid."

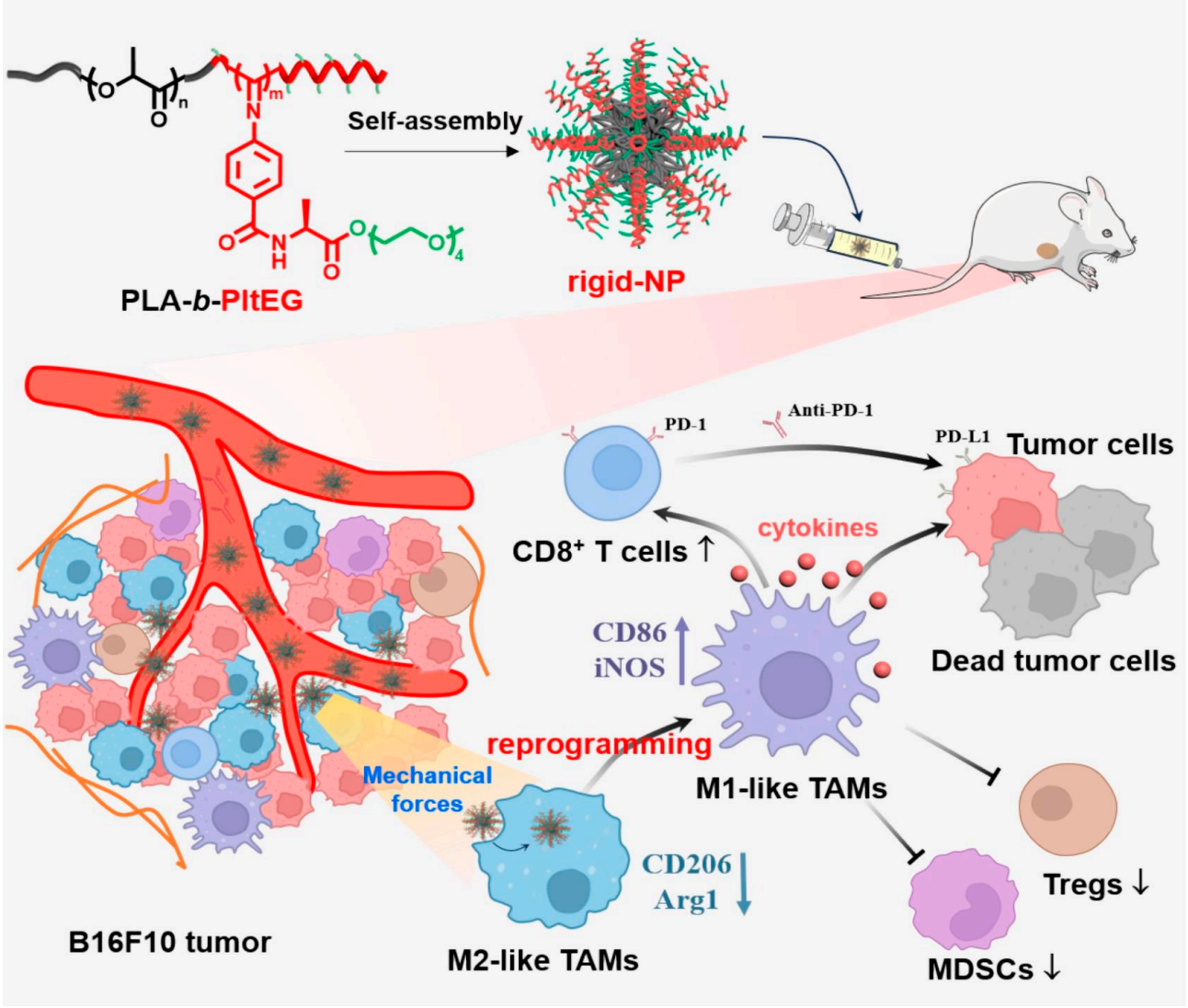

Figure 4. Intrinsic macrophage targeting by mechanical forces. Self-assembled rigid nanoparticles with helical polymer shells reprogrammed M2-like TAMs into an M1-like phenotype for tumor immunotherapy. Reprinted with permission from Ref. [108], 2024, Elsevier.

4. Localized Activation of Intrinsically Selective Nanoplatforms

The safety profile and therapeutic window of iNPs can be further improved by leveraging local cues and external triggers to enhance their selectivity and activity. These stimuli are classified into two categories: microenvironment-based chemical stimuli (e.g., local acidity and oxygen concentration), and physical stimuli (e.g., local temperature and artificially applied triggers).

4.1. Microenvironment-Responsive Selectivity

Microenvironment-responsive nanoparticles offer a non-toxic approach for targeting bacteria and tumors with enhanced precision by exploiting pH gradients in diseased tissues. Biofilms may produce an acidic microenvironment due to their metabolic activity [114]. Likewise, the tumor microenvironment (TME) is often acidic, which may contribute to the growth of many solid cancers [115]. Therefore, iNPs with activity limited to acidic microenvironments have been explored to treat and image both disease systems [116,117]. Strategies used in pH-sensitive nanoparticle design include the incorporation of partially ionizable chemical groups like amide (C=O-N-) and imide

(C=N-) bonds, which are protonated at acidic pH [118–121]. Multilayered nanoparticles comprising pH-dependent, hydrolysable polyelectrolyte polymeric chains have been developed to target negatively charged biofilms and undergo hydrolysis, which results in a positive surface charge and nanoparticle attraction to negatively charged biofilms (Figure 5) [122].

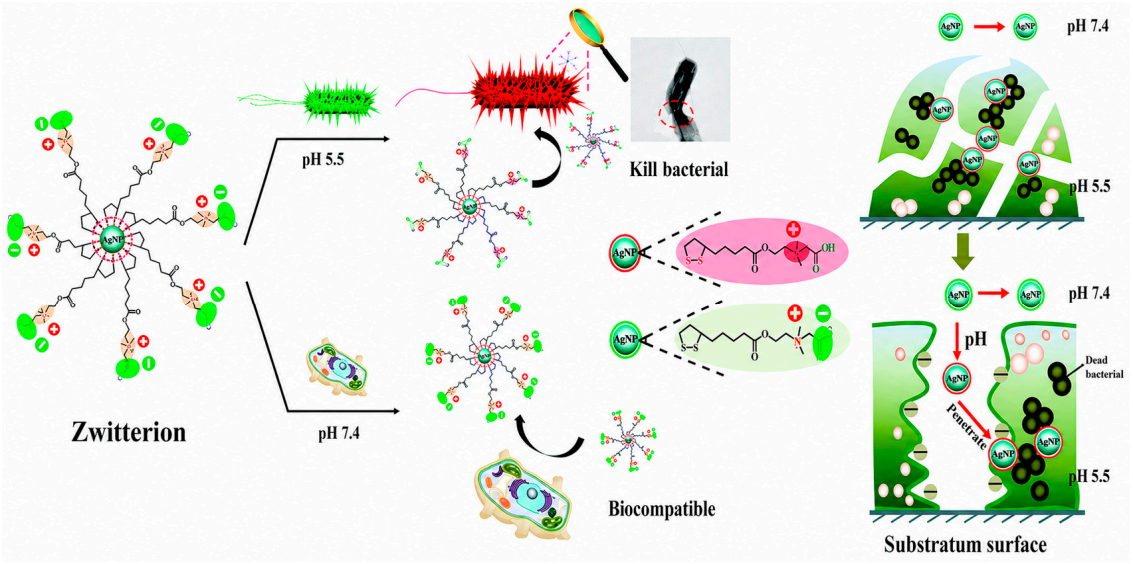

Figure 5. Intrinsic bacterial targeting via microenvironment selectivity. Zwitterion modified AgNPs showed a pH-responsive transition from a negative charge to a positive charge, which enabled the AgNPs to be compatible with mammalian cells and red blood cells (RBCs) in healthy tissues (pH ~ 7.4), while strongly adhering quickly to negatively charged bacterial surfaces at infectious sites (pH ~ 5.5) based on electrostatic attraction. Reprinted with permission from Ref. [122], 2019, Royal Society of Chemistry.

Redox-responsive drug delivery systems exploit the elevated glutathione (GSH) levels in tumors, which are four-fold higher than in healthy cells, creating a more reductive environment [123,124]. Other reducing agents like hydrogenated nicotinamide adenine dinucleotide phosphate (NADPH), gamma-interferon-inducible lysosomal thiol reductase enzyme (GILT), and thioredoxin also contribute to the tumor's reductive environment, further supporting controlled drug release. Redox-responsive iNPs can include disulfide bonds, diselenide bonds, succinimide-thioether linkages, and tetrasulfide bonds, with disulfide-containing platforms being most prevalent in liposomes, polymeric micelles, and nanogels [125]. The mechanism involves hydrogen donation from GSH's thiol group to the nanocarrier, breaking its structure and releasing anticancer drugs into the cytosol, where they are most effective. Disulfide bonds are particularly common due to rapid reduction by GSH and stability in blood circulation, ensuring drug release is localized at tumor sites to minimize side effects [126–128].

Enzyme-responsive nanoparticles exploit biochemical signatures of the target tissue by incorporating enzyme-sensitive coatings, cleavable linkers, or catalytic cascades to selectively release the therapeutic payload [129]. Tissues with characteristic enzymatic signatures that can be targeted with enzyme-responsive iNPs, include tumor microenvironments, gastrointestinal organs, regions of inflammation or infection, and the heart, to name a few [130–133]. For example, hybrid porous silicon nanoparticles with negative surface charge were shown to specifically target positively charged inflamed intestinal sites and preferentially accumulate there after oral administration [133]. The high concentration of lipase enzymes in the diseased intestines subsequently triggered localized payload release from the iNPs, thereby treating the target tissue with high selectivity.

As highlighted by this example, enzyme-responsive systems can be designed to work in conjunction with other stimulus-responsive approaches to enhance treatment selectivity and reduce non-specific activity.

4.2. Physical Stimulus-Responsive Selectivity

Physical external signals such as temperature, light, ultrasound, magnetic fields, and applied or endogenous mechanical force fields can be used to activate iNPs (Scheme 1). By confining activation to diseased tissues, these physical stimuli can achieve spatiotemporally controlled therapy and simultaneous imaging while minimizing off-target toxicity [134]. Mechanical-force-responsive systems are considered here alongside heat, light, ultrasound, and magnetism. The relevant stimulus may be externally applied force or an endogenous force field such as interstitial flow, vascular shear, tissue compression, or rheological confinement. These cues can alter particle margination, deformation, adhesion, permeability, or shell rupture, enabling flow-gated delivery in narrowed vessels, stress-enhanced penetration into dense tissues, or mechanically triggered release from soft carriers. In this sense, rheology is not merely a barrier to transport; it can be engineered as a selectivity filter that amplifies differences between healthy and diseased tissues [105–108,134–136].

Nanoplatforms that respond to temperature typically include thermoresponsive polymers that are able to undergo phase transitions at a defined lower critical solution temperature (LCST) or upper critical solution temperature (UCST) [137]. The LCST or UCST can trigger drug release or structural changes. Polymers such as poly(N-isopropylacrylamide) (PNIPAM) or oligo (ethylene glycol) -(OEG)-based copolymers are widely used, with their LCST tuned to a mild hyperthermia range of 40–43 °C to respond to tumors' pathologically elevated temperatures and localize payload delivery [137,138]. In cancer therapy, thermosensitive nanosystems can be activated by endogenous temperature differences between the tumor and normal tissue [139]. Hyperthermia can also be externally triggered by focused light or magnetic systems to release cargo at the selected site [140–142]. Hybrid design frequently combines the responsiveness to temperature along with other modalities such as magnetic or near-infrared (NIR) absorbing components, to enhance the selectivity and enable multimodal therapy and imaging [143].

Light-activated nanoplatforms exploit ultraviolet, visible, or NIR light to induce photochemical reactions (e.g., photocleavage and photoisomerization) and/or photodynamic effects that can trigger drug release or generate cytotoxic species locally [138,144]. NIR-responsive systems are particularly attractive because biological tissues scatter and absorb NIR less than visible light, enabling NIR penetration depths on the order of centimeters. Among other applications, NIR-responsive iNPs can be leveraged for the precise ablation of tumors via photothermal or photodynamic therapy [134]. iNPs can also embed photosensitizers, photochromic linkers, or plasmonic materials. For example, self-assembled nanoparticles composed of photosensitizer IR-780 and glutathione blocking agent CB-839 cloaked in a tumor cell membrane achieved inherent gastric adenocarcinoma targeting, and treated the tumor by metabolic reprogramming and laser-triggered photodynamic therapy [142]. Upon illumination, the light is converted into heat or reactive oxygen species within the irradiated region, minimizing systemic damage and improving therapeutic indices. When combined with imaging probes, these light-responsive nanoplatforms can function as theranostic systems, allowing real-time monitoring of accumulation and treatment response [72,140].

Ultrasound-responsive nanoparticles transduce mechanical and thermal effects into selective drug release, enhanced tissue penetration, or piezoelectric stimulation of local neural cells [135]. For example, $BaTiO_3$ nanoparticles with chitosan glycol shell were demonstrated to create electromagnetic fields upon ultrasonic treatment, showing promis-

ing ventricular rate control for atrial fibrillation treatment [145]. Other typical constructions include polymeric nanoparticles, liposomes, or micro/nanobubbles that are destabilized or fragmented under specific ultrasound frequencies, resulting in burst release of encapsulated cargos at the desired site [146]. Ultrasound is clinically established and can be focused deep within the tissues with good spatial resolution. Therefore, these platforms can support image-guided therapy, particularly when combined with echogenic components for contrast-enhanced ultrasound imaging [147,148]. Moreover, ultrasound can transiently increase vascular and cellular permeability, improving intratumoral penetration of drugs or genes delivered by these nanosystems [136].

Magnetic field-responsive nanoplatforms usually incorporate superparamagnetic iron oxide or related magnetic nanomaterials to enable field-guided targeting, magnetic hyperthermia, and magnetic resonance imaging (MRI). Under an alternating magnetic field, these nanoparticles generate localized heat that can both directly damage tumor cells and act as an internal trigger for temperature-sensitive matrices, producing synergistic magnetothermal drug release [134,138,140]. For example, magnetoliposome encapsulating magnetic nanoparticles (MZFs) and antitumor drugs (As_2O_3) intrinsically targeted liver tumors through the liposome's inherent liver tropism [141]. An alternating magnetic field was applied to induce magnetic hyperthermia and drug release, leading to synergistic antihepatoma effects in vitro and in vivo. Static magnetic fields can enhance the accumulation of magnetically responsive carriers at specific sites, whereas their intrinsic magnetic properties allow use as T_2 or T_1 MRI contrast agents, yielding integrated diagnosis and therapy in a single nanoplatform [82]. Multifunctional designs frequently combine magnetic responsiveness with other stimulus-sensitive components, such as pH or light, to better match the complexity of the TME and further refine spatiotemporal selectivity [138,143,149].

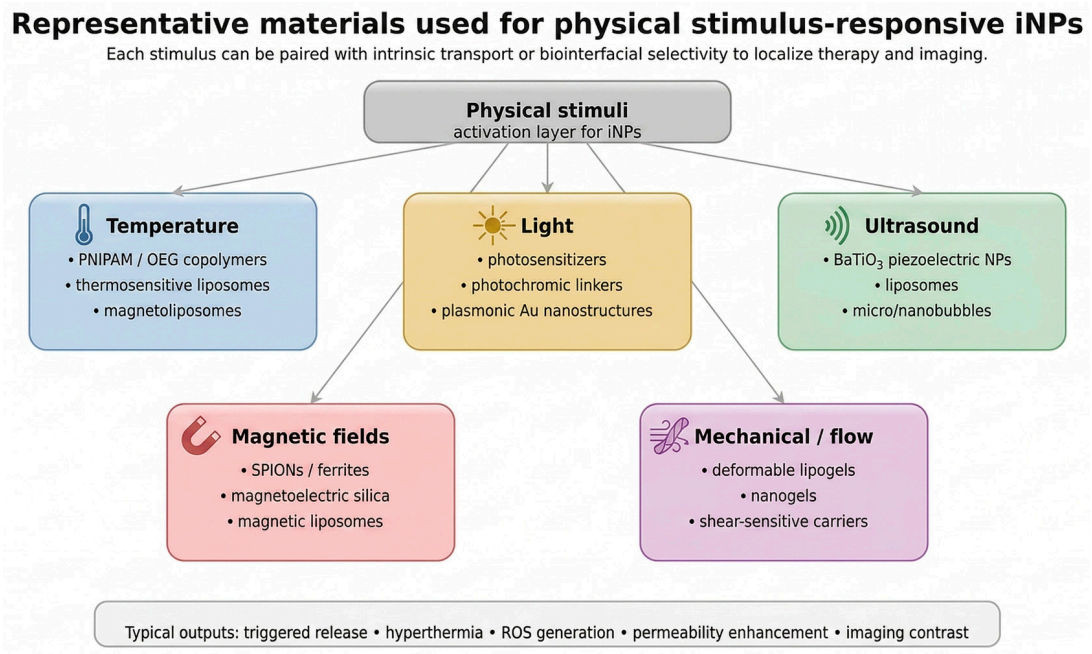

Scheme 1. Representative materials, transduction modes, and downstream outputs used for physical-stimulus-responsive intrinsically selective nanoplatforms. Thermoresponsive polymers and magnetoliposomes respond to heat; photosensitizers, photochromic linkers, and plasmonic gold nanostructures to light; piezoelectric ceramics, liposomes, and micro/nanobubbles to ultrasound; superparamagnetic iron oxide, ferrites, and magnetoelectric silica to magnetic fields; and deformable lipogels, nanogels, or shear-sensitive carriers to mechanical or rheological cues. Downstream outputs include triggered release, hyperthermia, ROS generation, permeability enhancement, and imaging contrast. Created for this review.

5. Therapeutic Applications

In practice, many successful iNPs combine intrinsic uptake biases with conditional activation to maximize selectivity in vivo. We now survey how these design principles have been implemented across therapeutic areas, emphasizing the disease-specific barriers each strategy addresses (Table 2).

Table 2. Representative therapeutic applications of intrinsically selective nanoplatforms, highlighting how selectivity, activation, and monitoring are combined in practice.

Disease	Representative iNP	Selectivity Mechanism	Optional Trigger or Added Selectivity	Monitoring/ Imaging	References
Cancer	Soft lipogels, magnetoelectric silica, TME-responsive carriers	Tumor mechanics, acidic/redox microenvironment, charge switching	Magnetic actuation, phototherapy, enzyme or hypoxia gating	Fluorescence, MRI, photoacoustics, thermal mapping	[82,83,105,140–142,150–159]
Bacterial infections	Zwitterionic AgNPs, cationic/charge-reversing liposomes, TiO_x@C	Anionic bacterial membranes, acidic biofilms, membrane stiffness/curvature	pH-triggered charge-reversal and biofilm penetration	Fluorescence or photoacoustic readouts in selected systems	[122,160–172]
Viral infections	Porous Au NPs, AgNPs, ZnO tetrapods	Viral surface protein chemistry and electrostatic capture	Endosomal acidification or immune-cell uptake	Surface-coating validation and viral-load reduction assays	[173–184]
Fungal infections	AmB–AgNPs, Cu-based NPs	Ergosterol-rich membranes and carboxyl-rich fungal walls	Redox stress and membrane destabilization	Primarily therapeutic; imaging remains limited	[185–189]
Cardiovascular disease	Macrophage membrane-coated PLGA; plaque-targeting carbon nanotubes	Inflammatory cell tropism and physicochemical uptake by plaque macrophages/monocytes	Local anti-inflammatory delivery	Photoacoustic imaging of plaques; MRI -compatible designs	[190–195]
Neurological disorders	MK16 LNPs, CNM-Au8, nanoceria	BBB transport tuned by lipid composition; metabolic or redox targeting	mRNA delivery, nanozyme activity, oxidative-stress buffering	Reporter expression, biodistribution imaging, neurofunctional readouts	[196–201]

Abbreviations: AgNPs, silver nanoparticles; ALS, amyotrophic lateral sclerosis; AmB, amphotericin B; BBB, blood–brain barrier; CT, computed tomography; iNPs, intrinsically selective nanoplatforms; LNPs, lipid nanoparticles; mRNA, messenger RNA; MRI, magnetic resonance imaging; NPs, nanoparticles; TME, tumor microenvironment.

5.1. Cancer Therapy

Despite great advances in cancer therapies, cancer remains difficult to treat, in part due to the intratumoral heterogeneity of cancer cells and their ability to adapt to stressors through mutations and epigenetic reprogramming [5,6]. Nanoparticles designed to intrinsically target cancer cells provide the advantage of bypassing the need for cell-surface biomarkers whose expression may be heterogeneous or downregulated over a treatment regimen. Strategies for intrinsic targeting take advantage of both the properties inherent to the nanomaterial and the abnormal biological conditions characteristic of tumors, including acidity, redox imbalance, enzyme activity, elevated interstitial pressure, dense extracellular matrix, and aberrant tissue mechanics [3,4,79,202,203]. Cancer cells are often mechanically softer than their healthy counterparts across many tumor types [204,205], therefore nanoparticle stiffness can be modulated to exploit these mechanical differences and improve tumor accumulation (Figure 6). More deformable carriers can prolong circulation and better negotiate constricted tumor interstitium, whereas stiffer constructs can strengthen membrane wrapping or engage macrophage mechanosensitive pathways, depending on formulation and target-cell state [105–108]. Intrinsic tumor targeting can also be enabled by pH-responsive degradation, enzyme-triggered release, redox sensitivity, and biomimetic membrane coatings, as described in previous sections [71,79,202,206–209]. In practice, many of these mechanisms overlap and can be combined within a single platform.

Overall, these varied approaches point toward a broader shift in nanoparticle design, building systems that work with tumor biology rather than requiring ligand specificity for targeting. The maturation of these systems holds promise for improving targeting precision, therapeutic reliability, and long-term clinical translation in nanotheranostic applications.

5.1.1. Magneto-Electric Systems

Nanoparticulate systems have been designed to target cancer cells using externally supplied magnetic fields to guide particles or trigger therapeutic payload release from the nanoplatforms. Intrinsic targeting of tumors was explored using magneto-electric silica nanoparticles which integrate magnetic control for payload delivery with the therapeutic behavior of metal-based components [82]. Rather than relying on molecular recognition, magneto-electric nanoparticles localize to tumors via interactions with the TME and on-demand zeta potential switching for cancer cell permeation [82,210,211]. Once internalized by cancer cells, the release of a therapeutic payload can be triggered by the application of an external AC magnetic field, which is conveniently possible with clinical MRI [82]. A related magnetic nanosystem couples chemotherapeutic delivery with photothermal therapy using gold-decorated core–shell Fe_3O_4@SiO_2 nanoparticles for magnetic targeting in non-small-cell lung cancer models [210]. From a practical standpoint, multifunctional designs with magnetic targeting capabilities help reduce systemic exposure while providing theranostic capabilities.

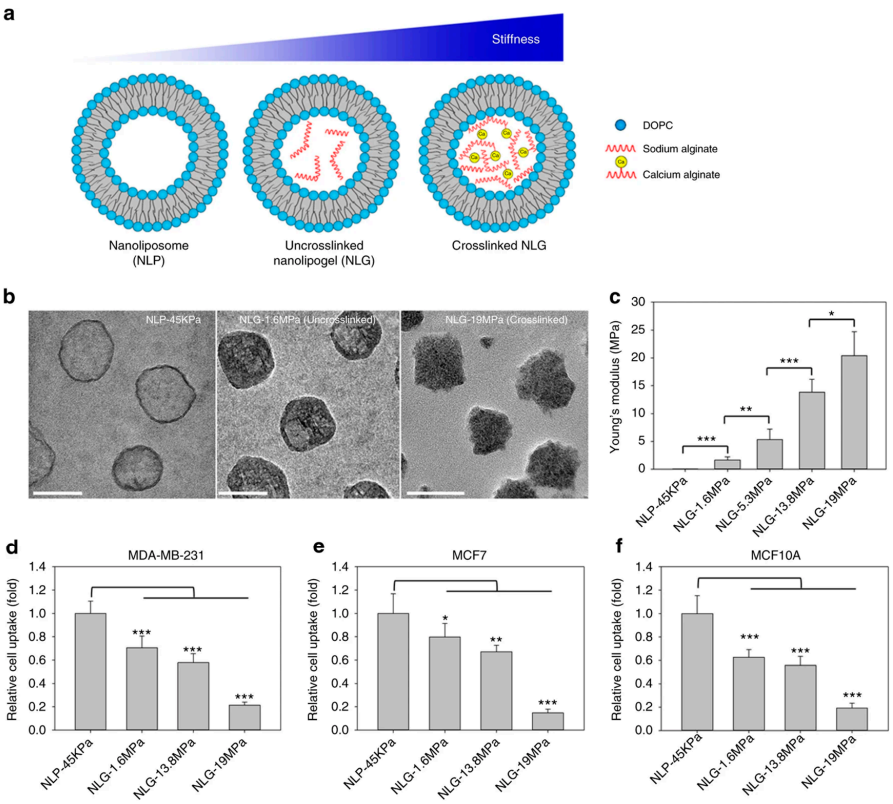

Figure 6. Inherent tumor cell targeting enabled by iNP mechanical properties. Particle elasticity regulates in vitro cellular uptake. (**a**) Schematic illustration of nanoliposome–hydrogel complex system. NLP represents nanoliposome encapsulating PBS. Uncrosslinked NLG represents nanoliposome encapsulating uncrosslinked alginate (0 mM $CaCl_2$). Crosslinked NLG represents nanolipogel encapsulating 1–5 mM $CaCl_2$ crosslinked alginate. (**b**) The internal structure of NPs with various elasticity (NLP-45 kPa, NLG-1.6 MPa, and NLG-19 MPa) characterized by TEM. Scale bars represent 100 nm. (**c**) The Young's moduli of synthesized NLP and NLGs characterized by AFM. Relative cellular uptake of synthesized NLP and NLGs by MDA-MB-231 (**d**), MCF7 (**e**), and MCF10A (**f**) cells. * $p < 0.05$, ** $p < 0.01$, *** $p < 0.001$. Adapted with permission from Ref. [105]. 2018, Springer Nature.

5.1.2. Environmental Targeting

In recent years, "smart" nanoparticles have been developed to remain inert until they encounter specific triggers. In oncology, environmental sensitivity can be leveraged to allow "smart" nanoparticles to exhibit activity confined to the TME, thereby only targeting diseased areas. Environmental triggers include, but are not limited to, enzymatic activity, pH, redox, hypoxia, and the presence of reactive oxygen species (ROS). Enzyme-responsive systems take advantage of the elevated activity of proteases, such as matrix metalloproteinases, and lipases, such as phospholipase A2, within the TME. Matrix metalloproteinases-2 (MMP-2) activatable nanoparticles have demonstrated non-permeability to normal tissues and uptake by tumor cells both in vitro and in vivo [150,151]. This selectivity has been applied to the intracellular delivery of proteins, chemotherapeutics, and antibodies, as well as tumor imaging, and has been deployed on cores composed of nickel ferrite, gold nanorods, and mesoporous silica, to name a few [150,151]. For example, an MMP-2-activated nanoparticle with a proteinase-sensitive cleavable linker tagged hyaluronic acid core was developed to deliver bispecific antibodies and epigallocatechin gallate across the blood–brain barrier to enhance immune checkpoint blockade therapy and induce ferroptosis in glioblastoma models in vivo [152].

Oxidation-reduction (redox) sensitive platforms activate in response to high intracellular glutathione levels and oxidative stress commonly exhibited by cancer cells [153]. Redox-responsive platforms can be formulated from a myriad of building blocks. Redox-responsive micelles, composed of amphiphilic glycan conjugates, have achieved targeted doxorubicin delivery and laryngopharyngeal cancer therapy in vitro [154]. Redox-responsive metal–organic framework nanocapsules were also leveraged for targeted drug release and triggered metabolic reprogramming of cancer cells [155]. A redox-responsive sialic acid (SA)-imprinted biodegradable silica nanoparticle was recently reported as a novel protein delivery strategy for targeted cancer therapy [156]. Last, a pH and redox-responsive hyperbranched polymeric nanocarrier selectively targeted breast cancer for docetaxel delivery [157].

Hypoxia-responsive iNPs exploit oxygen deprivation in tumors. Hypoxia-responsive azocalix[4]arene (AC4A) has been conjugated to human serum albumin-based nanoplatforms to treat hypoxic tumors, as hypoxia triggers conformational changes in AC4A, leading to drug delivery [158]. Similarly, hypoxia-responsive nanoparticles of copolymeric 4-nitrobenzyl (3-azidopropyl) carbamate and mPEG-PPLG were found to effectively release doxorubicin into cancer cell nuclei in vitro and to mitigate the side effects of the drug in vivo [159].

5.2. Antimicrobial Therapies

In contrast to oncology, where selectivity often exploits the tumor microenvironment, antimicrobial iNPs frequently leverage conserved differences in membrane charge, curvature, and mechanical stiffness between microbes and host cells to achieve broad activity with reduced host toxicity.

5.2.1. Bacterial Infections

Given the extensive application of nanomaterials in combating bacterial infections, many recent innovations have focused on minimizing cytotoxic effects for healthy mammalian cells [160]. A well-established strategy exploits the electrostatic attraction between silver-based nanoparticles (AgNPs) and negatively charged bacterial membranes [160,161], with particular efficacy against Gram-negative bacteria [162,163]. This intrinsic physical targeting enables AgNPs to circumvent common resistance mechanisms, furthering the importance of AgNPs as antibacterial agents [160]. However, unmodified AgNPs also

interact with the negatively charged components of mammalian cell membranes, resulting in unacceptable host toxicity. Modifications such as PEGylation, and membrane oxidation have been employed to reduce nonspecific cytotoxicity [122,173]. Another innovation was the incorporation of pH-responsive zwitterions into AgNPs, enabling a transition from a biocompatible, negatively charged state to a positively charged antibacterial state localized at infection sites due to the inherently acidic bacterial environment [122].

Liposomes remain a widely used platform to direct antibiotics to bacterial infections, enabling dose reduction and thus lowering the selective pressure in which antibiotic resistance can develop [160]. Liposomes are particularly advantageous for targeting biofilms, which are difficult to eradicate with conventional therapies [164,165]. Incorporation of cationic lipids confers intrinsic bacterial targeting [166–168], although the lipid composition and chain length must be carefully engineered to balance antibacterial efficacy against host cytotoxicity [167]. Alternatively, ionizable, charge-reversing lipids may be incorporated into liposomes to ensure biocompatibility during circulation and activation into an intrinsically selective cationic form only upon encountering a bacterial microenvironment [169].

Some of the most promising innovations to improve selectivity exploit fundamental biophysical differences between bacterial and mammalian cell membranes. Linear cationic polymers exhibit electrostatic attraction to both membrane types, but remain non-toxic until assembly into nanoparticles which preferentially disrupt bacterial membranes. This selectivity emerges from interactions with bacterial negative-curvature lipids that promote pore formation and leakage of intracellular contents, while mammalian membranes enriched in zero-curvature lipids resist disruption [170,171]. Similarly, TiO_x@C nanoparticles, comprising a carbon substrate decorated with titanium dioxide dots, specifically penetrated the relatively stiff bacterial cell membranes, while cholesterol within the eukaryotic cell membranes prevented the TiO_x@C nanoparticles from disrupting the eukaryotic cell membrane (Figure 7) [172].

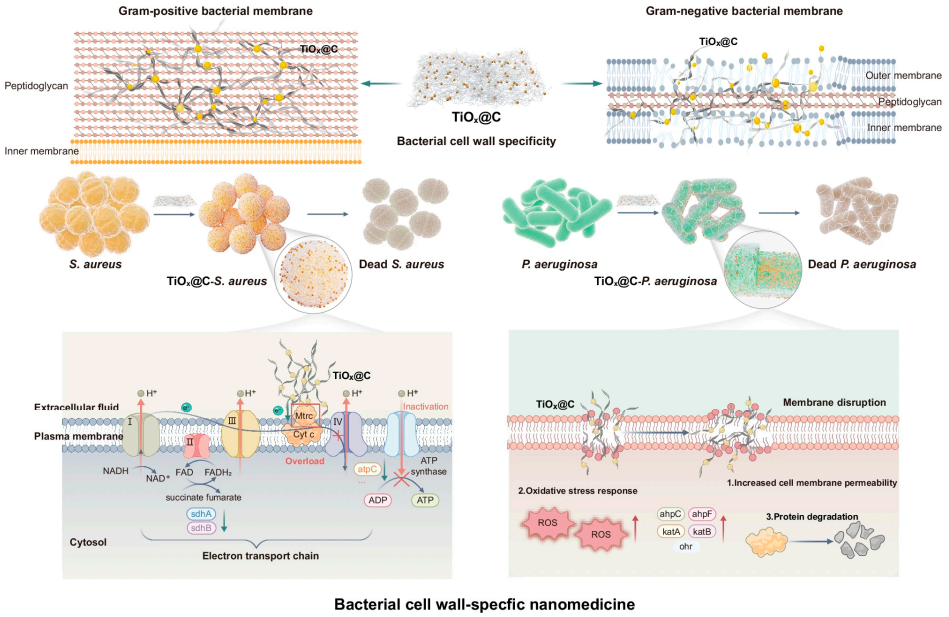

Figure 7. Exploiting differences in bacterial and eukaryotic cell membranes provides routes for intrinsic selectivity. The fiber-like carbon substrate of TiOx@C nanoparticle is capable of selectively entangling with the peptidoglycan layer of *S. aureus*, further disrupting the electron transport chain and killing the bacteria by delivering excess electrons to key enzymes of the electron transport chain via TiOx dots. Meanwhile, the carbon substrate of TiOx@C penetrated the cell wall of *P. aeruginosa*, disrupted the bacterial membrane structure and penetrated the bacteria, and triggered oxidative stress and protein leakage, thus leading to bacterial death. Reprinted with permission from Ref. [172], 2025, Springer Nature.

5.2.2. Viral Infections

Intrinsic targeting strategies for antiviral nanoparticles aim to disrupt interactions between viral surfaces and host cell receptors. Nanoparticles may be engineered to mimic viral ligand properties, competitively binding host receptors and preventing viral attachment [174,175]. Alternatively, electrostatic and chemical interactions enable direct targeting of viral proteins [174,176–178]. For example, porous gold nanoparticles have extensive surface area to engage in gold-thiol interactions, facilitating disulfide bond cleavage in viral proteins and thus reducing the ability of the pathogen to establish infection while maintaining mammalian biocompatibility [176,179]. AgNPs similarly target sulfhydryl groups, both on viral surface proteins and host cell glycoproteins, to inhibit viral attachment [180,181], and also interfere with viral replication by binding to viral nucleic acids or nucleocapsids [174,180,181]. As with antibacterial AgNPs, however, successful in vivo application requires modifications to minimize mammalian cytotoxicity [173,180]. Zinc oxide tetrapod nanoparticles are shown to capture viral bodies and promote engulfment of pathogen/nanoparticle complexes by immunological cells [182]. Antiviral surface coatings have also been shown to reduce viral load on high touch surfaces [183,184], such as fluorinated titanium oxide nanoparticles that induce oxidative stress under fluorescent lighting [184].

5.2.3. Fungal Infections

Intrinsic antifungal targeting presents greater challenges due to close eukaryotic similarity with mammalian cells. Although AgNPs have gained widespread use, continued innovation is required to enhance selectivity and biocompatibility [162]. Copper-based nanoparticles have emerged as a less toxic alternative, preferentially adhering to carboxyl-rich fungal cell walls, leading to membrane destabilization, reactive oxygen species generation, and disruption of enzymatic pathways [185,186]. Recent studies demonstrated the feasibility of discriminating between ergosterol-rich membranes, as in fungi, and cholesterol-dominant mammalian cells for targeted antifungal delivery. For instance, AgNPs conjugated with amphotericin B (AmB) exhibited preferential binding to ergosterol in parasitic membranes, resulting in enhanced eradication and reduced mammalian cytotoxicity, relative to free AmB [187]. This approach is supported by studies showing that AmB-loaded nanocarriers against *Candida albicans* lowered the minimum inhibitory concentration of required antibiotic and reduced hemolysis [188,189], indicating that such an approach might be employed effectively against fungal infections.

5.3. Cardiovascular Diseases

Intrinsic selectivity principles are increasingly being adapted to chronic non-communicable diseases, where vascular barriers, inflammatory trafficking, and tissue-specific extracellular matrices strongly influence delivery, including cardiovascular diseases. Current focus is on nanoplatforms that improve targeting capabilities and overcome biological barriers [190]. Furthermore, novel biomimetic membrane-coated nanoparticles are gaining traction to achieve highly targeted amelioration of conditions like pressure overload-induced cardiac fibrosis [191]. Macrophage membrane-coated drug delivery systems, comprising lutein-loaded PLGA nanoparticle cores coated with macrophage membrane are emerging as a possible treatment for hypertensive heart disease (HHD) [191]. The macrophage membranes provide protection from phagocytosis by immune cells, granting longer circulation times, [191,192] which, coupled with the ability to easily load drugs onto PLGA cores, make these biomimetic nanoparticles strong for HHD and other possible cardiovascular diseases in the future [84]. Other areas of research include intrinsic atherosclerotic plaque targeting for imaging, which is highly challenging with typical techniques such as MRI and CT due to the small size of coronary vessels, rapid

heart motion, and the difficulty to differentiate soft, non-calcified, or lipid-rich plaque components. Plaque inflammation is characterized by an abundance of immune cells in the arterial wall, mainly foamy macrophages and their progenitors, inflammatory Ly-6C^{hi} monocytes [193,194]. These two immune cell types characteristic of plaque can be intrinsically targeted using carbon nanotubes, whose physicochemistry allows them to exclusively accumulate in these two cell types [195]. The carbon nanotube iNPs have been successfully leveraged to photoacoustically image inflamed atherosclerotic plaques with precision, and demonstrate the potential of iNPs for cardiovascular theranostic applications.

5.4. Neurological Disorders

Neurological disorders remain challenging to target due to the challenges posed by the blood–brain barrier (BBB)—not only a physical hurdle, the BBB actively pumps xenobiotics back into the bloodstream after they cross using efflux pumps including P-glycoprotein (P-gp) [196]. Despite these challenges, several nanoparticle strategies have been leveraged to intrinsically target several neurological disorders. Recent studies are highlighted by MK16, a specialized lipid nanoparticle that successfully traversed the BBB in murine models to deliver therapeutic mRNA, effectively reversing memory deficits [197]. The lipid shell is composed of ionizable lipids, cholesterol, and PEG-lipids, which can promote BBB transport by increasing endocytosis signaling in caveolae, and protecting the encapsulated mRNA until reaching target brain cells by encapsulating it in a protective lipid barrier [197]. Nanoparticle treatments for Amyotrophic Lateral Sclerosis (ALS) have progressed further with clinical translation of a gold nanocrystal therapy, termed CNM-Au8 after the company name Clene Nanomedicine, currently under evaluation for ALS treatment [198]. CNM-Au8 functions as an NADH dehydrogenase-mimicking nanozyme that regulates energy metabolism [199]. This unique property makes the nanocrystal a candidate for supporting central nervous system bioenergetics and for strengthening central nervous system cells. Nanoceria are another promising platform for the intrinsic targeting of neurological disorders. Their intrinsic redox activity allows them to directly target and treat oxidative stress which is a central driver of neurodegeneration in diseases like Huntington's, Alzheimer's, and Parkinson's [200], and is also common in ischemic, hemorrhagic, and traumatic brain injuries [201].

6. Diagnostic and Monitoring Capabilities

A key advantage of many iNPs is that they can simultaneously report on delivery and response, either through intrinsic contrast (e.g., magnetic or optical signatures) or by co-loading imaging agents. This section highlights diagnostic modalities and monitoring strategies that enable real-time theranostic feedback.

6.1. Imaging Modalities

Imaging modalities that are widely used for nanoplatform visualization and characterization include fluorescence imaging, magnetic resonance imaging (MRI), computed tomography imaging (CT), and photoacoustic imaging. Long-standing clinical and preclinical use of these modalities enables extensive diagnostic and monitoring capabilities for nanoplatforms.

Fluorescence imaging is widely accessible, as many nanoplatforms can be readily functionalized with fluorophores. In vitro fluorescence studies are routinely used to assess target cell localization [82,169,212] and cellular uptake [213], by incorporating fluorophores either on the nanoplatform surface or within the carrier. Similarly, these techniques have been optimized for in vitro data collection. Localization to the disease site and cellular uptake in vitro are well-established uses of fluorescence imaging [80,214,215]. Environment-

responsive platforms further enable monitoring of therapy payload release following cellular internalization [213,216].

MRI generates contrast through differences in the proton excitation and relaxation potential of tissues, and most soft tissues require exogenous contrast agents for clinically relevant imaging [217]. As previously discussed, magnetic nanoparticles often exhibit intrinsic T_2 or T_1 MRI contrast, with iron oxide, cobalt ferrite, and manganese oxide producing T_2-weighted contrast [82,90,218]. These nanoparticles retain contrast functionality after surface modification and can be engineered to remain in a non-contrasting form until internalized by target cells [219].

Much like MRI, CT imaging also benefits from nanomaterials with high X-ray attenuation, such as iron oxide, gold, hafnium oxide, and barium dysprosium nanoparticles [220–222]. In vivo biodistribution of nanoparticles is possible with CT imaging, which provides data on targeted tissue uptake and elimination half-life, as is the case for zirconium oxide nanoparticles [223]. Ligand-free targeted nanoplatforms with surface functionalization can enhance visualization of tumor sites or create contrast greater than conventional iodine-based contrast agents [224–226]. Non-iodine nanoparticle-based contrast agents are also beneficial due to the potential for decreased doses, decrease in renal toxicity, and increase in blood circulation time [226,227].

Photoacoustic imaging generates data when target tissues absorb emitted light, thermally expand, and produce ultrasound waves due to expansion and contraction [228]. Since its emergence in the early 2000s, this modality has gained increasing interest for diagnostic and therapeutic monitoring [229–231]. Nanomaterials with strong optical absorption, such as gold nanorods, have enabled thermal mapping and validation of temperature profiles in tumor thermal therapy [232].

The combination of multiple imaging modalities provides complementary structural, functional, and thermal information. By layering images of soft and hard tissues with temperature maps, treatment efficacy can be monitored [233]. Multimodal nanoplatforms, such as Gd metal−organic framework nanoparticles hybridized with gold nanoparticles, or barium dysprosium create high MRI and CT contrast [222,234]. Combined MRI, photoacoustic, and Raman imaging has clinical applications in surgery to delineate tumor boundaries from healthy tissue (Figure 8) [235].

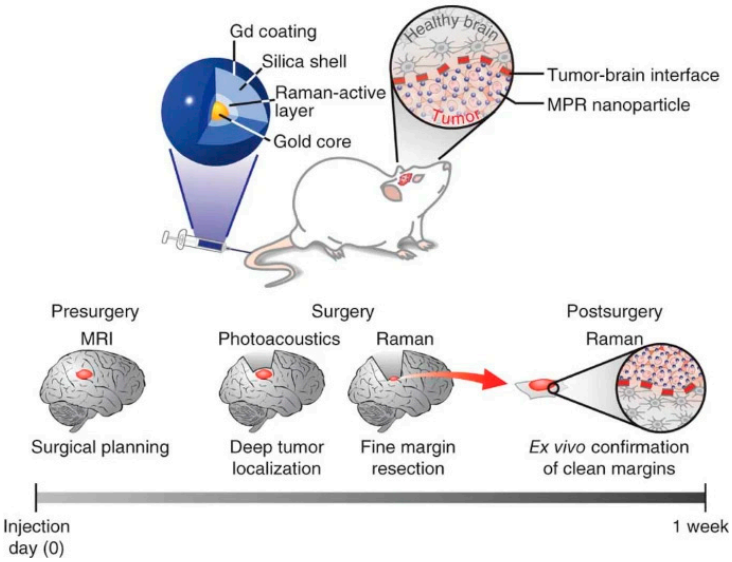

Figure 8. Triple-modality magnetic resonance imaging–photoacoustic imaging–Raman imaging nanoparticle (MPR) can accurately delineate the margins of brain tumors in living mice both preoperatively and intraoperatively. The MPRs were detected by all three modalities with at least a picomolar sensitivity both in vitro and in living mice. Reprinted with permission from Ref. [235], 2012, Springer Nature.

6.2. Real-Time Monitoring

Imaging modalities such as fluorescence, MRI, and CT can be used for real-time monitoring of nanoplatform-mediated therapies, including treatment response, biodistribution, accumulation, and circulation half-life [82,215,223,236]. Photoacoustic imaging, for example, in combination with nanoplatforms, allows for verification that therapeutic temperature thresholds are met during the therapy [232,237,238]. In vivo monitoring of nanoplatform distribution informs targeting efficiency and optimal treatment timing. Researchers can exploit the properties of their nanoplatforms to release an imaging probe once the therapy has been encapsulated by the target tissue and the therapeutic product is released [213].

6.3. Theranostic Integration

Theranostics integrate diagnosis and therapy within a single platform. Nanoplatforms are well-suited for theranostics due to offering co-delivery of therapeutic payloads and imaging agents while also providing tunable pharmacokinetics and surface chemistry. Intrinsically selective nanomaterials can reduce reliance on precise pre-identification of disease markers by leveraging physiological or biophysical signatures of diseased tissue. For example, coupling chemotherapy with thermal therapies (e.g., photothermal therapy or magnetic hyperthermia) can help delineate disease margins while simultaneously ablating tumor tissue [216,239]. Image-guided therapies combine an imaging modality with a treatment to provide visualization during intervention. These approaches use imaging modalities such as MRI, fluorescence, or photoacoustic imaging to locate tumors and determine boundaries, and then treat with photodynamic therapy, thermal therapy, or surgical resection [214,240,241]. Gold nanoparticles and magnetic iron oxide nanoparticles have been used to assist thermal ablation by targeting tumor cells and mapping temperature profiles at the tumor site with the use of optical backscattered reflectometry [237,238]. In addition to light-mediated photothermal strategies, magnetic nanoparticles can enable magnetic hyperthermia or magnetic ablation under alternating magnetic fields, offering deep-tissue heating that can be paired with MRI-compatible treatment planning and monitoring [57,242,243].

7. Future Perspectives and Emerging Directions

7.1. Clinical Translation Challenges and Opportunities

Therapeutic monitoring has an important and direct impact on translation by providing real-time feedback on dose selection, safety assessment, and patient stratification. We therefore discuss clinical progress and key regulatory considerations specific to ligand-free and stimulus-responsive nanotheranostics. Most intrinsically selective (ligand-free) platforms are still preclinical, but clinical momentum is emerging from formulations that exploit disease physiology rather than affinity ligands. Tumor-acidity/charge-switching carriers [37,78,213], protein-corona-guided delivery concepts [7,236], and externally actuated magnetic strategies [218,244] represent translationally plausible motifs for pairing therapy with imaging or pharmacokinetic readouts. However, label-free targeting is context dependent: EPR and vascular permeability vary across patients; microenvironment triggers (pH, enzymes, hypoxia) are heterogeneous; and corona composition shifts with plasma proteomes and disease state, making it difficult to produce a homogeneous response among all patients [8,9]. For biomimetic coatings, scale-up and storage can alter membrane proteins that mediate homotypic adhesion and immune evasion [87,91,93]. Safety issues include immunogenicity, complement activation, long-term inorganic retention, and off-target heating for externally driven platforms.

In the U.S. and EU, nanoplatforms are reviewed as drugs/biologics, devices, or combination products depending on the primary mode of action (chemical payload vs physical energy deposition vs diagnostic function). Sponsors must define critical quality attributes (size/shape distributions, surface chemistry/charge, loading and release, sterility/endotoxin), validate assays for stability and corona behavior, and show that intrinsic selectivity improves a meaningful clinical endpoint (response, survival, or validated diagnostic performance), not only biodistribution.

Although not explicitly engineered for intrinsic selectivity, approved liposomes, albumin nanocarriers, and lipid nanoparticles show that complex nanosystems can satisfy chemistry, manufacturing, and controls, plus pharmacovigilance expectations and reach broad adoption. These precedents suggest a pragmatic path for intrinsically selective nanotheranostics: simplify compositions, integrate companion monitoring, and apply quality-by-design to lock in surface features that drive reproducible selectivity.

7.2. Emerging Directions

Finally, we look ahead to emerging directions that could improve reproducibility and personalization of intrinsic selectivity, including data-driven design, multi-input "logic" gating, and tighter integration of delivery with real-time monitoring.

Artificial intelligence and machine learning will increasingly convert "trial-and-error" nanomedicine into a data-driven workflow. Models trained on physicochemical descriptors can predict protein-corona fingerprints, biodistribution, and clearance, enabling rational use of corona engineering to steer targeting [7–9]. Coupled to automated microfluidic synthesis and active learning, AI can iteratively propose and test formulations that maximize selectivity while constraining toxicity and manufacturability. Generative models and digital twins can pre-specify feasible design spaces for quality-by-design.

Beyond single triggers (e.g., pH), the next wave will use multi-input "logic" responses: charge-reversal plus enzyme cleavage, hypoxia-activated phototherapy, or redox-gated drug release. Biomimetic interfaces may evolve from single-cell membrane cloaks to hybrid or modular coatings (tumor + immune cell membranes) that combine homotypic adhesion with immune evasion [91,93]. Materials that adapt their stiffness, shape, or aggregation state in situ could add a biophysical layer of label-free selectivity relevant to tumors, biofilms, and inflamed tissues.

Intrinsically selective nanoplatforms are well-positioned to deliver next-generation payloads (mRNA, CRISPR editors, protein degraders) and to interface with energy-based medicine (focused ultrasound, photothermal/photodynamic therapy, magnetic actuation). Integrating real-time imaging (photoacoustic, MRI, fluorescence) with closed-loop control can enable dose-painting and on-the-fly adjustment of therapy. Pairing nanotheranostics with wearable sensors could further connect delivery to systemic response.

Personalization will move from "one nanoparticle fits all" to patient-adaptive design: screening formulations in a patient's own plasma to anticipate corona effects; using imaging to quantify delivery and adjust dosing; and even deriving membranes or vesicles from patient tumors for autologous homotypic targeting. Finally, multi-omics biomarkers and AI-based stratification can identify which patients are most likely to benefit from a given intrinsic-selectivity mechanism.

8. Conclusions

Intrinsically selective nanoplatforms (iNPs) provide a compelling route to precise therapy and monitoring when classical ligand–receptor targeting is impractical, unreliable, or vulnerable to heterogeneity and adaptive resistance. Across inorganic, organic, and hybrid material classes, this review highlights how inherent physicochemical and biophysical properties such as size/shape, surface charge and charge-switching behavior, mechanical stiffness, membrane biomimetics, and metabolism/organelle biases enable preferential localization and uptake in diseased tissues without requiring a predefined molecular marker. iNPs can improve selectivity through localized activation, either by microenvironmental cues (e.g., acidity, redox state, enzymatic activity, hypoxia) or by externally applied physical stimuli (e.g., light, temperature, ultrasound, magnetic fields), enabling spatiotemporally controlled therapy with reduced off-target exposure. Importantly, many iNPs support theranostic coupling by integrating imaging readouts (fluorescence, MRI, CT, photoacoustic imaging) that quantify delivery, activation, and treatment response in real time.

These capabilities directly advance the goals of precision medicine. By reducing dependence on static biomarkers and leveraging disease-state physiology, iNPs broaden eligibility for patients whose tumors or infections lack stable targets, and offer practical pathways to adaptive dosing informed by imaging-confirmed accumulation and response. Theranostic monitoring also supports patient stratification (who is likely to accumulate/activate a platform), optimization of treatment timing, and the emergence of closed-loop "dose-painting" strategies that adjust therapy based on measurable in vivo signals. More broadly, intrinsic selectivity mechanisms are particularly attractive for complex, heterogeneous disease contexts—such as solid tumors, biofilms, and inflamed tissues—where molecular signatures evolve under therapeutic pressure.

Despite rapid progress, several challenges must be addressed for translation. Intrinsic selectivity is context-dependent: vascular permeability, microenvironment triggers, and protein corona composition vary across patients, disease stages, and anatomical sites, complicating reproducibility. Externally actuated platforms require careful control of energy deposition and safety margins, while biomimetic coatings introduce scale-up, storage, and batch-consistency constraints. Across all classes, regulators will expect robust definition of critical quality attributes (size/shape distributions, surface chemistry/charge, loading and release behavior), validated assays that correlate "intrinsic" properties with clinical performance, and long-term safety datasets addressing immunogenicity, complement activation, and persistence/clearance.

Looking forward, the most promising opportunities lie in multi-input "logic-gated" designs (combining intrinsic uptake biases with conditional activation), corona and interface engineering to stabilize in vivo behavior, and AI/ML-guided formulation discovery linked to automated synthesis and quality-by-design manufacturing. Together, these strategies position iNPs as a practical foundation for next-generation, patient-adaptive nanotheranostics.

Author Contributions: Conceptualization: A.F.B., P.D.N.; Validation: A.F.B., R.K.R., P.D.N.; Formal analysis: A.F.B.; Investigation: A.F.B., P.D.N.; Resources: P.D.N.; Data curation: A.F.B., C.K., H.H.W., S.W., P.L., R.E., O.S., J.L., R.D., V.H., P.D.N.; Writing—original draft preparation: A.F.B., C.K., H.H.W., S.W., P.L., R.E., O.S., J.L., R.D., V.H., P.D.N.; Writing—review and editing: A.F.B., R.K.R., P.D.N.; Visualization: A.F.B., P.D.N.; Supervision: A.F.B., P.D.N.; Project administration: P.D.N.; Funding acquisition: P.D.N.; All authors have read and agreed to the published version of the manuscript.

Funding: The personnel effort for compiling this review article was funded in the Nallathamby lab by a CDMRP-PRCRP IDEA award (HT94252510332). The Nallathamby lab would like to acknowledge the financial and material support of the Notre Dame Berthiaume Institute for Precision Health (BIPH), and the Notre Dame Center for Nanoscience and Technology (NDnano) undergraduate research fellowships. Shirley Wei, Philip Latorre, Ryan Eastland, Olivia Sayani, Jichong Lyu, Ryan Davey, and Victoria Hopkins were undergraduate research associates. Shirley Wei, Olivia Sayani, Ryan Davey, and Victoria Hopkins were funded by the NDnano Undergraduate Research Fellowship (NURF). Jichong Lyu was funded by the NDnano Undergraduate Research Fellowship (NURF) and the Harper Cancer Research Institute's Summer Undergraduate Research Fellowship. Aurelie Brownsberger was funded by the Notre Dame Materials Science and Engineering Program Graduate Fellowship. Hezekiah Williams was funded by the Jack and Mary Ann Remick Fellowship. Research efforts in the Nallathamby lab were also supported by a Project Development Team grant from the Indiana Clinical and Translational Sciences Institute (CTSI-PDT: 373037-31005-FY19CTSIK), Institutional Research Grants from the American Cancer Society (ACS IRG-17-182-04, ACS IRG-17-182-04-2), and seed grants from the Notre Dame Berthiaume Institute for Precision Health (372333-31025) and (372717-43310-FY17RFP).

Data Availability Statement: No new data were created or analyzed in this study. Data sharing is not applicable to this article.

Conflicts of Interest: The authors declare no conflicts of interest.

References

1. Maeda, H. Toward a Full Understanding of the EPR Effect in Primary and Metastatic Tumors as Well as Issues Related to Its Heterogeneity. *Adv. Drug Deliv. Rev.* **2015**, *91*, 3–6. [CrossRef]
2. Fang, J.; Nakamura, H.; Maeda, H. The EPR Effect: Unique Features of Tumor Blood Vessels for Drug Delivery, Factors Involved, and Limitations and Augmentation of the Effect. *Adv. Drug Deliv. Rev.* **2011**, *63*, 136–151. [CrossRef]
3. Nia, H.T.; Liu, H.; Seano, G.; Datta, M.; Jones, D.; Rahbari, N.; Incio, J.; Chauhan, V.P.; Jung, K.; Martin, J.D.; et al. Solid Stress and Elastic Energy as Measures of Tumour Mechanopathology. *Nat. Biomed. Eng.* **2016**, *1*, 0004. [CrossRef]
4. Yi, X.; Jin, X.; Hu, Y.; Shen, Z.; Zheng, X.; Luo, D.; Xu, T.; Yan, J.; Huang, P. Drug Delivery Systems for Overcoming Physical Barriers in Cancer Therapy. *Mol. Pharm.* **2025**, *22*, 6413–6429. [CrossRef]
5. Hanahan, D.; Weinberg, R.A. Hallmarks of Cancer: The Next Generation. *Cell* **2011**, *144*, 646–674. [CrossRef]
6. Hanahan, D. Hallmarks of Cancer: New Dimensions. *Cancer Discov.* **2022**, *12*, 31–46. [CrossRef]
7. Kim, W.; Ly, N.K.; He, Y.; Li, Y.; Yuan, Z.; Yeo, Y. Protein Corona: Friend or Foe? Co-Opting Serum Proteins for Nanoparticle Delivery. *Adv. Drug Deliv. Rev.* **2023**, *192*, 114635. [CrossRef] [PubMed]
8. Bashiri, G.; Padilla, M.S.; Swingle, K.L.; Shepherd, S.J.; Mitchell, M.J.; Wang, K. Nanoparticle Protein Corona: From Structure and Function to Therapeutic Targeting. *Lab Chip* **2023**, *23*, 1432–1466. [CrossRef] [PubMed]
9. Singh, N.; Marets, C.; Boudon, J.; Millot, N.; Saviot, L.; Maurizi, L. In Vivo Protein Corona on Nanoparticles: Does the Control of All Material Parameters Orient the Biological Behavior? *Nanoscale Adv.* **2021**, *3*, 1209–1229. [CrossRef]
10. He, Y.; Wang, Y.; Wang, L.; Jiang, W.; Wilhelm, S. Understanding Nanoparticle-Liver Interactions in Nanomedicine. *Expert Opin. Drug Deliv.* **2024**, *21*, 829–843. [CrossRef] [PubMed]
11. Fang, R.H.; Kroll, A.V.; Gao, W.; Zhang, L. Cell Membrane Coating Nanotechnology. *Adv. Mater.* **2018**, *30*, 1706759. [CrossRef]
12. Sebastiani, F.; Yanez Arteta, M.; Lerche, M.; Porcar, L.; Lang, C.; Bragg, R.A.; Elmore, C.S.; Krishnamurthy, V.R.; Russell, R.A.; Darwish, T.; et al. Apolipoprotein E Binding Drives Structural and Compositional Rearrangement of mRNA-Containing Lipid Nanoparticles. *ACS Nano* **2021**, *15*, 6709–6722. [CrossRef] [PubMed]
13. Mohri, K.; Miyazaki, T.; Warashina, S.; Takahashi, M.; Ren, Q.; Iida, R.; Wada, Y.; Maeda, K.; Watanabe, Y.; Suzuki, Y.; et al. Positron Emission Tomography-Based Pharmacokinetics of mRNA-Lipid Nanoparticles: A Study Quantifying the ApoE and Macrophage Contribution. *ACS Appl. Mater. Interfaces* **2025**, *17*, 45625–45639. [CrossRef]
14. Wang, H.; Wang, Q.; Dong, J.; Jiang, W.; Kong, L.; Zhang, Q.; Liu, H. New Perspective of Ceria Nanodots for Precise Tumor Therapy via Oxidative Stress Pathway. *Heliyon* **2022**, *8*, e10370. [CrossRef]
15. Diaconeasa, Z.; Rugină, D.; Coman, C.; Socaciu, C.; Leopold, L.F.; Vulpoi, A.; Tăbăran, F.; Suciu, M.; Mesaroş, A.; Popa, L.M.; et al. New Insights Regarding the Selectivity and the Uptake Potential of Nanoceria by Human Cells. *Colloids Surf. Physicochem. Eng. Asp.* **2017**, *532*, 132–139. [CrossRef]

16. Lu, M.; Zhang, Y.; Wang, Y.; Jiang, M.; Yao, X. Insight into Several Factors That Affect the Conversion Between Antioxidant and Oxidant Activities of Nanoceria. *ACS Appl. Mater. Interfaces* **2016**, *8*, 23580–23590. [CrossRef]
17. Tang, J.L.Y.; Moonshi, S.S.; Ta, H.T. Nanoceria: An Innovative Strategy for Cancer Treatment. *Cell. Mol. Life Sci.* **2023**, *80*, 46. [CrossRef]
18. Saifi, M.A.; Peddakkulappagari, C.S.; Ahmad, A.; Godugu, C. Leveraging the Pathophysiological Alterations of Obstructive Nephropathy to Treat Renal Fibrosis by Cerium Oxide Nanoparticles. *ACS Biomater. Sci. Eng.* **2020**, *6*, 3563–3573. [CrossRef]
19. Lakshmanan, M.; Saini, M.; Nune, M. Exploring the Innovative Application of Cerium Oxide Nanoparticles for Addressing Oxidative Stress in Ovarian Tissue Regeneration. *J. Ovarian Res.* **2024**, *17*, 241. [CrossRef] [PubMed]
20. Olton, D.Y.E.; Close, J.M.; Sfeir, C.S.; Kumta, P.N. Intracellular Trafficking Pathways Involved in the Gene Transfer of Nano-Structured Calcium Phosphate-DNA Particles. *Biomaterials* **2011**, *32*, 7662–7670. [CrossRef] [PubMed]
21. Kiss, A.L.; Botos, E. Endocytosis via Caveolae: Alternative Pathway with Distinct Cellular Compartments to Avoid Lysosomal Degradation? *J. Cell. Mol. Med.* **2009**, *13*, 1228–1237. [CrossRef] [PubMed]
22. Chao, Y.-W.; Lee, Y.-L.; Tseng, C.-S.; Wang, L.U.-H.; Hsia, K.-C.; Chen, H.; Fustin, J.-M.; Azeem, S.; Chang, T.-T.; Chen, C.-Y.; et al. Improved CaP Nanoparticles for Nucleic Acid and Protein Delivery to Neural Primary Cultures and Stem Cells. *ACS Nano* **2024**, *18*, 4822–4839. [CrossRef]
23. Zhang, K.; Zhou, Y.; Xiao, C.; Zhao, W.; Wu, H.; Tang, J.; Li, Z.; Yu, S.; Li, X.; Min, L.; et al. Application of Hydroxyapatite Nanoparticles in Tumor-Associated Bone Segmental Defect. *Sci. Adv.* **2019**, *5*, eaax6946. [CrossRef]
24. Mao, W.; Yoo, H.S. Inorganic Nanoparticle Functionalization Strategies in Immunotherapeutic Applications. *Biomater. Res.* **2024**, *28*, 0086. [CrossRef] [PubMed]
25. Yu, F.; Wang, H.; Wang, Q.; Zhai, F.; Wang, J.; Huang, C.; Cui, L. Studies of a Novel Bone-Targeted Nano Drug Delivery System with a HAP Core-PSI Coating Structure for Tanshinol Injection. *J. Drug Target.* **2023**, *31*, 762–775. [CrossRef]
26. Zhang, Q.; Qiang, L.; Liu, Y.; Fan, M.; Si, X.; Zheng, P. Biomaterial-Assisted Tumor Therapy: A Brief Review of Hydroxyapatite Nanoparticles and Its Composites Used in Bone Tumors Therapy. *Front. Bioeng. Biotechnol.* **2023**, *11*, 1167474. [CrossRef]
27. Maia, A.L.C.; Cavalcante, C.H.; Souza, M.G.F.d.; Ferreira, C.d.A.; Rubello, D.; Chondrogiannis, S.; Cardoso, V.N.; Ramaldes, G.A.; Barros, A.L.B.d.; Soares, D.C.F. Hydroxyapatite Nanoparticles: Preparation, Characterization, and Evaluation of Their Potential Use in Bone Targeting: An Animal Study. *Nucl. Med. Commun.* **2016**, *37*, 775. [CrossRef]
28. Kettenberger, U.; Luginbuehl, V.; Procter, P.; Pioletti, D.P. In Vitro and in Vivo Investigation of Bisphosphonate-Loaded Hydroxyapatite Particles for Peri-Implant Bone Augmentation. *J. Tissue Eng. Regen. Med.* **2017**, *11*, 1974–1985. [CrossRef] [PubMed]
29. Kong, D.; Chen, Z. Evaluation of the Interaction between Hydroxyapatite and Bisphosphonate by Nonlinear Capillary Electrochromatography. *J. Sep. Sci.* **2017**, *40*, 2030–2036. [CrossRef]
30. Wu, V.M.; Mickens, J.; Uskoković, V. Bisphosphonate-Functionalized Hydroxyapatite Nanoparticles for the Delivery of the Bromodomain Inhibitor JQ1 in the Treatment of Osteosarcoma. *ACS Appl. Mater. Interfaces* **2017**, *9*, 25887–25904. [CrossRef]
31. Rawat, P.; Manglani, K.; Gupta, S.; Kalam, A.; Vohora, D.; Ahmad, F.J.; Talegaonkar, S. Design and Development of Bioceramic Based Functionalized PLGA Nanoparticles of Risedronate for Bone Targeting: In-Vitro Characterization and Pharmacodynamic Evaluation. *Pharm. Res.* **2015**, *32*, 3149–3158. [CrossRef]
32. Rawat, P.; Ahmad, I.; Thomas, S.C.; Pandey, S.; Vohora, D.; Gupta, S.; Ahmad, F.J.; Talegaonkar, S. Revisiting Bone Targeting Potential of Novel Hydroxyapatite Based Surface Modified PLGA Nanoparticles of Risedronate: Pharmacokinetic and Biochemical Assessment. *Int. J. Pharm.* **2016**, *506*, 253–261. [CrossRef]
33. Wang, Y.; Zhou, Y.; Zhai, D.; Deng, H.; Chen, X. Design and in Vitro Evaluation of ^{223}Ra/^{99m}Tc-Loaded Spherical Nano-Hydroxyapatite in Bone Tumor Therapy. *Nanomedicine* **2024**, *19*, 1557–1567. [CrossRef]
34. Zhai, D.; Wang, Y.; Yu, S.; Zhou, J.; Song, J.; Hao, S.; Chen, X. Design and Evaluation of ^{32}P-Labeled Hydroxyapatite Nanoparticles for Bone Tumor Therapy. *Drug Deliv.* **2023**, *30*, 2168791. [CrossRef]
35. Chakraborty, S.; Das, T.; Sarma, H.D.; Venkatesh, M.; Banerjee, S. Preparation and Preliminary Studies on ^{177}Lu-Labeled Hydroxyapatite Particles for Possible Use in the Therapy of Liver Cancer. *Nucl. Med. Biol.* **2008**, *35*, 589–597. [CrossRef] [PubMed]
36. Wang, Y.; He, L.; Yu, B.; Chen, Y.; Shen, Y.; Cong, H. ZnO Quantum Dots Modified by pH-Activated Charge-Reversal Polymer for Tumor Targeted Drug Delivery. *Polymers* **2018**, *10*, 1272. [CrossRef] [PubMed]
37. Zhang, P.; Chen, D.; Li, L.; Sun, K. Charge Reversal Nano-Systems for Tumor Therapy. *J. Nanobiotechnol.* **2022**, *20*, 31. [CrossRef]
38. Yao, C.; Tu, Y.; Ding, L.; Li, C.; Wang, J.; Fang, H.; Huang, Y.; Zhang, K.; Lu, Q.; Wu, M.; et al. Tumor Cell-Specific Nuclear Targeting of Functionalized Graphene Quantum Dots In Vivo. *Bioconjug. Chem.* **2017**, *28*, 2608–2619. [CrossRef] [PubMed]
39. Park, S.Y.; Tan, J.K.S.; Mo, X.; Song, Y.; Lim, J.; Liew, X.R.; Chung, H.; Kim, S. Carbon Quantum Dots with Tunable Size and Fluorescence Intensity for Development of a Nano-Biosensor. *Small* **2025**, *21*, 2404524. [CrossRef]
40. Noh, J.; Kim, H.G.; Houck, D.W.; Shah, T.; Zhang, Y.; Brumberg, A.; Schaller, R.D.; Korgel, B.A. Colloidal Germanium Quantum Dots with Broadly Tunable Size and Light Emission. *J. Am. Chem. Soc.* **2025**, *147*, 1792–1802. [CrossRef]
41. Huang, W.; Wang, S.; Gong, H.; Tian, J.; Peng, J.; Cao, J. Size Tunable and Controllable Synthesis of PbS Quantum Dots for Broadband Photoelectric Response. *Opt. Mater.* **2023**, *142*, 113977. [CrossRef]

42. Coey, J.M.D.; Khalafalla, D. Superparamagnetic γ-Fe_2O_3. *Phys. Status Solidi A* **1972**, *11*, 229–241. [CrossRef]
43. Martins, C.; Rolo, C.; Cacho, V.R.G.; Pereira, L.C.J.; Borges, J.P.; Silva, J.C.; Vieira, T.; Soares, P.I.P. Enhancing the Magnetic Properties of Superparamagnetic Iron Oxide Nanoparticles Using Hydrothermal Treatment for Magnetic Hyperthermia Application. *Mater. Adv.* **2025**, *6*, 1726–1743. [CrossRef]
44. Dulińska-Litewka, J.; Łazarczyk, A.; Hałubiec, P.; Szafrański, O.; Karnas, K.; Karewicz, A. Superparamagnetic Iron Oxide Nanoparticles—Current and Prospective Medical Applications. *Materials* **2019**, *12*, 617. [CrossRef] [PubMed]
45. Sarma, L.; Aomoa, N.; Sarmah, T.; Sarma, S.; Srinivasan, A.; Sharma, G.; Gupta, A.; Reddy, V.R.; Satpati, B.; Srivastava, D.N.; et al. Synthesis of Finest Superparamagnetic Carbon-Encapsulated Magnetic Nanoparticles by a Plasma Expansion Method for Biomedical Applications. *J. Alloys Compd.* **2018**, *749*, 768–775. [CrossRef]
46. Davydov, V.; Rakhmanina, A.; Kireev, I.; Alieva, I.; Zhironkina, O.; Strelkova, O.; Dianova, V.; Samani, T.D.; Mireles, K.; Yahia, L.H.; et al. Solid State Synthesis of Carbon-Encapsulated Iron Carbide Nanoparticles and Their Interaction with Living Cells. *J. Mater. Chem. B* **2014**, *2*, 4250–4261. [CrossRef] [PubMed]
47. Liu, Z.; Lin, H.; Zhao, M.; Dai, C.; Zhang, S.; Peng, W.; Chen, Y. 2D Superparamagnetic Tantalum Carbide Composite MXenes for Efficient Breast-Cancer Theranostics. *Theranostics* **2018**, *8*, 1648–1664. [CrossRef]
48. Zhang, Y.; Zhou, J.; Luo, K.; Zhou, W.; Wang, F.; Li, J.; He, Q. Ferritin-Inspired Encapsulation and Stabilization of Gold Nanoclusters for High-Performance Photothermal Conversion. *Angew. Chem. Int. Ed.* **2025**, *64*, e202500058. [CrossRef]
49. Zhu, Y.; Zhu, Y.; Cao, T.; Liu, X.; Liu, X.; Yan, Y.; Shi, Y.; Wang, J.-C. Ferritin-Based Nanomedicine for Disease Treatment. *Med. Rev.* **2023**, *3*, 49–74. [CrossRef]
50. Neusch, A.; Wiedwald, U.; Novoselova, I.P.; Kuckla, D.A.; Tetos, N.; Sadik, S.; Hagemann, P.; Farle, M.; Monzel, C. Semisynthetic Ferritin-Based Nanoparticles with High Magnetic Anisotropy for Spatial Magnetic Manipulation and Inductive Heating. *Nanoscale* **2024**, *16*, 15113–15127. [CrossRef]
51. Ma, K.; Xu, S.; Tao, T.; Qian, J.; Cui, Q.; Rehman, S.U.; Zhu, X.; Chen, R.; Zhao, H.; Wang, C.; et al. Magnetosome-Inspired Synthesis of Soft Ferrimagnetic Nanoparticles for Magnetic Tumor Targeting. *Proc. Natl. Acad. Sci. USA* **2022**, *119*, e2211228119. [CrossRef] [PubMed]
52. Peigneux, A.; Jabalera, Y.; Vivas, M.A.F.; Casares, S.; Azuaga, A.I.; Jimenez-Lopez, C. Tuning Properties of Biomimetic Magnetic Nanoparticles by Combining Magnetosome Associated Proteins. *Sci. Rep.* **2019**, *9*, 8804. [CrossRef] [PubMed]
53. Rosenfeldt, S.; Mickoleit, F.; Jörke, C.; Clement, J.H.; Markert, S.; Jérôme, V.; Schwarzinger, S.; Freitag, R.; Schüler, D.; Uebe, R.; et al. Towards Standardized Purification of Bacterial Magnetic Nanoparticles for Future in Vivo Applications. *Acta Biomater.* **2021**, *120*, 293–303. [CrossRef]
54. Tonga, G.Y.; Moyano, D.F.; Kim, C.S.; Rotello, V.M. Inorganic Nanoparticles for Therapeutic Delivery: Trials, Tribulations and Promise. *Curr. Opin. Colloid Interface Sci.* **2014**, *19*, 49–55. [CrossRef]
55. Cho, E.C.; Glaus, C.; Chen, J.; Welch, M.J.; Xia, Y. Inorganic Nanoparticle-Based Contrast Agents for Molecular Imaging. *Trends Mol. Med.* **2010**, *16*, 561–573. [CrossRef]
56. Delille, F.; Pu, Y.; Lequeux, N.; Pons, T. Designing the Surface Chemistry of Inorganic Nanocrystals for Cancer Imaging and Therapy. *Cancers* **2022**, *14*, 2456. [CrossRef]
57. Shakeri-Zadeh, A.; Bulte, J.W.M. Imaging-Guided Precision Hyperthermia with Magnetic Nanoparticles. *Nat. Rev. Bioeng.* **2025**, *3*, 245–260. [CrossRef] [PubMed]
58. Vassallo, M.; Martella, D.; Barrera, G.; Celegato, F.; Coïsson, M.; Ferrero, R.; Olivetti, E.S.; Troia, A.; Sözeri, H.; Parmeggiani, C.; et al. Improvement of Hyperthermia Properties of Iron Oxide Nanoparticles by Surface Coating. *ACS Omega* **2023**, *8*, 2143–2154. [CrossRef]
59. Rezaei, B.; Mostufa, S.; Azizi, E.; Wang, Y.A.; Li, C.; Gómez-Pastora, J.; He, R.; Wu, K. Investigation on the Magnetic Hyperthermia Performance of Commercial Iron Oxide Magnetic Nanoparticles. *IEEE Trans. Magn.* **2025**, *61*, 5400305. [CrossRef]
60. Mekuye, B.; Abera, B. Nanomaterials: An Overview of Synthesis, Classification, Characterization, and Applications. *Nano Sel.* **2023**, *4*, 486–501. [CrossRef]
61. Mitragotri, S.; Patrick, S. Organic Nanoparticles for Drug Delivery and Imaging. *MRS Bull.* **2014**, *39*, 219–223. [CrossRef]
62. Jiang, Z.; Liu, H.; He, H.; Yadava, N.; Chambers, J.J.; Thayumanavan, S. Anionic Polymers Promote Mitochondrial Targeting of Delocalized Lipophilic Cations. *Bioconjug. Chem.* **2020**, *31*, 1344–1353. [CrossRef]
63. Mashima, R.; Takada, S. Lipid Nanoparticles: A Novel Gene Delivery Technique for Clinical Application. *Curr. Issues Mol. Biol.* **2022**, *44*, 5013–5027. [CrossRef]
64. Polack, F.P.; Thomas, S.J.; Kitchin, N.; Absalon, J.; Gurtman, A.; Lockhart, S.; Perez, J.L.; Marc, G.P.; Moreira, E.D.; Zerbini, C.; et al. Safety and Efficacy of the BNT162b2 mRNA COVID-19 Vaccine. *N. Engl. J. Med.* **2020**, *383*, 2603–2615. [CrossRef]
65. Cafri, G.; Gartner, J.J.; Hopson, K.; Meehan, R.S.; Zaks, T.Z.; Robbins, P.; Rosenberg, S.A. Immunogenicity and Tolerability of Personalized mRNA Vaccine mRNA-4650 Encoding Defined Neoantigens Expressed by the Autologous Cancer. *J. Clin. Oncol.* **2019**, *37*, 2643. [CrossRef]

66. Herrera, M.; Kim, J.; Eygeris, Y.; Jozic, A.; Sahay, G. Illuminating Endosomal Escape of Polymorphic Lipid Nanoparticles That Boost mRNA Delivery. *Biomater. Sci.* **2021**, *9*, 4289–4300. [CrossRef]
67. Sun, D.; Lu, Z.-R. Structure and Function of Cationic and Ionizable Lipids for Nucleic Acid Delivery. *Pharm. Res.* **2023**, *40*, 27–46. [CrossRef]
68. Hou, X.; Zaks, T.; Langer, R.; Dong, Y. Lipid Nanoparticles for mRNA Delivery. *Nat. Rev. Mater.* **2021**, *6*, 1078–1094. [CrossRef]
69. Ryals, R.C.; Patel, S.; Acosta, C.; McKinney, M.; Pennesi, M.E.; Sahay, G. The Effects of PEGylation on LNP Based mRNA Delivery to the Eye. *PLoS ONE* **2020**, *15*, e0241006. [CrossRef]
70. Vasileva, O.; Zaborova, O.; Shmykov, B.; Ivanov, R.; Reshetnikov, V. Composition of Lipid Nanoparticles for Targeted Delivery: Application to mRNA Therapeutics. *Front. Pharmacol.* **2024**, *15*, 1466337. [CrossRef]
71. Badparvar, F.; Marjani, A.P.; Salehi, R.; Ramezani, F. pH/Redox Responsive Size-switchable Intelligent Nanovehicle for Tumor Microenvironment Targeted DOX Release. *Sci. Rep.* **2023**, *13*, 22475. [CrossRef]
72. Chang, D.; Ma, Y.; Xu, X.; Xie, J.; Ju, S. Stimuli-Responsive Polymeric Nanoplatforms for Cancer Therapy. *Front. Bioeng. Biotechnol.* **2021**, *9*, 707319. [CrossRef]
73. Hu, C.-M.J.; Zhang, L.; Aryal, S.; Cheung, C.; Fang, R.H.; Zhang, L. Erythrocyte Membrane-Camouflaged Polymeric Nanoparticles as a Biomimetic Delivery Platform. *Proc. Natl. Acad. Sci. USA* **2011**, *108*, 10980–10985. [CrossRef]
74. Eltaib, L. Polymeric Nanoparticles in Targeted Drug Delivery: Unveiling the Impact of Polymer Characterization and Fabrication. *Polymers* **2025**, *17*, 833. [CrossRef]
75. Cho, H.; Lai, T.C.; Tomoda, K.; Kwon, G.S. Polymeric Micelles for Multi-Drug Delivery in Cancer. *AAPS PharmSciTech* **2015**, *16*, 10–20. [CrossRef]
76. Zhang, Z.; Xiong, X.; Wan, J.; Xiao, L.; Gan, L.; Feng, Y.; Xu, H.; Yang, X. Cellular Uptake and Intracellular Trafficking of PEG-*b*-PLA Polymeric Micelles. *Biomaterials* **2012**, *33*, 7233–7240. [CrossRef]
77. Nelemans, L.C.; Gurevich, L.; Nelemans, L.C.; Gurevich, L. Drug Delivery with Polymeric Nanocarriers—Cellular Uptake Mechanisms. *Materials* **2020**, *13*, 366. [CrossRef]
78. Jin, Z.; Jin, M.; Jiang, C.; Yin, X.; Jin, S.; Quan, X.; Gao, Z. Evaluation of Doxorubicin-Loaded pH-Sensitive Polymeric Micelle Release from Tumor Blood Vessels and Anticancer Efficacy Using a Dorsal Skin-Fold Window Chamber Model. *Acta Pharmacol. Sin.* **2014**, *35*, 839–845. [CrossRef]
79. Palanikumar, L.; Al-Hosani, S.; Kalmouni, M.; Nguyen, V.P.; Ali, L.; Pasricha, R.; Barrera, F.N.; Magzoub, M. pH-Responsive High Stability Polymeric Nanoparticles for Targeted Delivery of Anticancer Therapeutics. *Commun. Biol.* **2020**, *3*, 95. [CrossRef]
80. Cheng, R.; Meng, F.; Deng, C.; Klok, H.-A.; Zhong, Z. Dual and Multi-Stimuli Responsive Polymeric Nanoparticles for Programmed Site-Specific Drug Delivery. *Biomaterials* **2013**, *34*, 3647–3657. [CrossRef]
81. Meng, F.; Zhong, Y.; Cheng, R.; Deng, C.; Zhong, Z. Ph-Sensitive Polymeric Nanoparticles for Tumor-Targeting Doxorubicin Delivery: Concept and Recent Advances. *Nanomedicine* **2014**, *9*, 487–499. [CrossRef]
82. Waters, M.; Hopf, J.; Tam, E.; Wallace, S.; Chang, J.; Bennett, Z.; Aquino, H.; Roeder, R.K.; Helquist, P.; Stack, M.S.; et al. Biocompatible, Multi-Mode, Fluorescent, T_2 MRI Contrast Magnetoelectric-Silica Nanoparticles (MagSiNs), for On-Demand Doxorubicin Delivery to Metastatic Cancer Cells. *Pharmaceuticals* **2022**, *15*, 1216. [CrossRef]
83. Lyu, J.; Brownsberger, A.F.; Kudary, C.; Waters, M.; Nallathamby, P. Receptor Independent Magnetoelectric Nanocarriers for Spatiotemporally Controlled Chemotherapy of Triple Negative Breast Cancer Variants, Ovarian Cancer, and Prostate Cancer. *ChemRxiv* **2025**. [CrossRef]
84. Vijayan, V.; Uthaman, S.; Park, I.-K. Cell Membrane Coated Nanoparticles: An Emerging Biomimetic Nanoplatform for Targeted Bioimaging and Therapy. *Adv. Exp. Med. Biol.* **2018**, *1064*, 45–59. [CrossRef]
85. Zeng, Y.; Li, S.; Zhang, S.; Wang, L.; Yuan, H.; Hu, F. Cell Membrane Coated-Nanoparticles for Cancer Immunotherapy. *Acta Pharm. Sin. B* **2022**, *12*, 3233–3254. [CrossRef]
86. Oroojalian, F.; Beygi, M.; Baradaran, B.; Mokhtarzadeh, A.; Shahbazi, M.-A. Immune Cell Membrane-Coated Biomimetic Nanoparticles for Targeted Cancer Therapy. *Small* **2021**, *17*, 2006484. [CrossRef]
87. Guo, Q.; Wang, S.; Xu, R.; Tang, Y.; Xia, X. Cancer Cell Membrane-Coated Nanoparticles: A Promising Anti-Tumor Bionic Platform. *RSC Adv.* **2024**, *14*, 10608–10637. [CrossRef]
88. Wen, H.; Poutiainen, P.; Batnasan, E.; Latonen, L.; Lehto, V.-P.; Xu, W. Biomimetic Inorganic Nanovectors as Tumor-Targeting Theranostic Platform against Triple-Negative Breast Cancer. *Pharmaceutics* **2023**, *15*, 2507. [CrossRef]
89. Rodrigues, C.F.; Correia, I.J.; Moreira, A.F. Red Blood Cell Membrane-Camouflaged Gold-Core Silica Shell Nanorods for Cancer Drug Delivery and Photothermal Therapy. *Int. J. Pharm.* **2024**, *655*, 124007. [CrossRef]
90. Wei, X.; Gao, J.; Fang, R.H.; Luk, B.T.; Kroll, A.V.; Dehaini, D.; Zhou, J.; Kim, H.W.; Gao, W.; Lu, W.; et al. Nanoparticles Camouflaged in Platelet Membrane Coating as an Antibody Decoy for the Treatment of Immune Thrombocytopenia. *Biomaterials* **2016**, *111*, 116–123. [CrossRef]
91. Fang, R.H.; Hu, C.-M.J.; Luk, B.T.; Gao, W.; Copp, J.A.; Tai, Y.; O'Connor, D.E.; Zhang, L. Cancer Cell Membrane-Coated Nanoparticles for Anticancer Vaccination and Drug Delivery. *Nano Lett.* **2014**, *14*, 2181–2188. [CrossRef]

92. Chen, Z.; Zhao, P.; Luo, Z.; Zheng, M.; Tian, H.; Gong, P.; Gao, G.; Pan, H.; Liu, L.; Ma, A.; et al. Cancer Cell Membrane-Biomimetic Nanoparticles for Homologous-Targeting Dual-Modal Imaging and Photothermal Therapy. *ACS Nano* **2016**, *10*, 10049–10057. [CrossRef] [PubMed]
93. Harris, J.C.; Scully, M.A.; Day, E.S. Cancer Cell Membrane-Coated Nanoparticles for Cancer Management. *Cancers* **2019**, *11*, 1836. [CrossRef]
94. Gu, C.; Yang, S.; Liu, X.; Jin, Y.; Yu, Y.; Lu, L. A Biomimetic Adipocyte Mesenchymal Stem Cell Membrane-Encapsulated Drug Delivery System for the Treatment of Rheumatoid Arthritis. *Nano Res.* **2023**, *16*, 11401–11410. [CrossRef]
95. Murphy, M.P.; Hartley, R.C. Mitochondria as a Therapeutic Target for Common Pathologies. *Nat. Rev. Drug Discov.* **2018**, *17*, 865–886. [CrossRef]
96. Xu, J.; Shamul, J.G.; Kwizera, E.A.; He, X. Recent Advancements in Mitochondria-Targeted Nanoparticle Drug Delivery for Cancer Therapy. *Nanomaterials* **2022**, *12*, 743. [CrossRef]
97. Džajić, I.; Tomašič, T.; Pardo, L.A.; Mašič, L.P.; Cotman, A.E. Lipophilic Cations as Mitochondria-Targeting Moieties: Recent Progress and Design Principles for Medicinal Chemistry. *J. Med. Chem.* **2025**, *68*, 23690–23704. [CrossRef]
98. Pathak, R.K.; Kolishetti, N.; Dhar, S. Targeted Nanoparticles in Mitochondrial Medicine. *Wiley Interdiscip. Rev. Nanomed. Nanobiotechnol.* **2015**, *7*, 315–329. [CrossRef]
99. Weissig, V.; Lizano, C.; Torchilin, V.P. Micellar Delivery System for Dequalinium—A Lipophilic Cationic Drug with Anticarcinoma Activity. *J. Liposome Res.* **1998**, *8*, 391–400. [CrossRef]
100. Liberti, M.V.; Locasale, J.W. The Warburg Effect: How Does It Benefit Cancer Cells? *Trends Biochem. Sci.* **2016**, *41*, 211–218. [CrossRef] [PubMed]
101. Li, Z.; Munim, M.B.; Sharygin, D.A.; Bevis, B.J.; Vander Heiden, M.G. Understanding the Warburg Effect in Cancer. *Cold Spring Harb. Perspect. Med.* **2025**, *15*, a041532. [CrossRef]
102. Kröger, A.P.P.; Komil, M.I.; Hamelmann, N.M.; Juan, A.; Stenzel, M.H.; Paulusse, J.M.J. Glucose Single-Chain Polymer Nanoparticles for Cellular Targeting. *ACS Macro Lett.* **2019**, *8*, 95–101. [CrossRef]
103. Kröger, A.P.P.; Hamelmann, N.M.; Juan, A.; Lindhoud, S.; Paulusse, J.M.J. Biocompatible Single-Chain Polymer Nanoparticles for Drug Delivery—A Dual Approach. *ACS Appl. Mater. Interfaces* **2018**, *10*, 30946–30951. [CrossRef]
104. Mahon, C.S.; McGurk, C.J.; Watson, S.M.D.; Fascione, M.A.; Sakonsinsiri, C.; Turnbull, W.B.; Fulton, D.A. Molecular Recognition-Mediated Transformation of Single-Chain Polymer Nanoparticles into Crosslinked Polymer Films. *Angew. Chem. Int. Ed. Engl.* **2017**, *56*, 12913–12918. [CrossRef]
105. Guo, P.; Liu, D.; Subramanyam, K.; Wang, B.; Yang, J.; Huang, J.; Auguste, D.T.; Moses, M.A. Nanoparticle Elasticity Directs Tumor Uptake. *Nat. Commun.* **2018**, *9*, 130. [CrossRef]
106. Sun, J.; Zhang, L.; Wang, J.; Feng, Q.; Liu, D.; Yin, Q.; Xu, D.; Wei, Y.; Ding, B.; Shi, X.; et al. Tunable Rigidity of (Polymeric Core)–(Lipid Shell) Nanoparticles for Regulated Cellular Uptake. *Adv. Mater.* **2015**, *27*, 1402–1407. [CrossRef]
107. Cao, Y.; Wong, Y.S.; Ben Mabrouk, A.; Anita, V.; Jie Liew, M.W.; Tan, Y.F.; Venkatraman, S.S. Nanolipogels as a Cell-Mimicking Platform for Controlled Release of Biomacromolecules. *Nanoscale Adv.* **2020**, *2*, 1040–1045. [CrossRef] [PubMed]
108. Zhang, Z.; Peng, Y.; Qiu, L. Rigid Nanoparticles for Efficient Tumor Immunotherapy through Mechanical Force Mediated Reprogramming of Tumor-Associated Macrophages. *Chem. Eng. J.* **2024**, *491*, 152129. [CrossRef]
109. Choi, H.S.; Ashitate, Y.; Lee, J.H.; Kim, S.H.; Matsui, A.; Insin, N.; Bawendi, M.G.; Semmler-Behnke, M.; Frangioni, J.V.; Tsuda, A. Rapid Translocation of Nanoparticles from the Lung Airspaces to the Body. *Nat. Biotechnol.* **2010**, *28*, 1300–1303. [CrossRef] [PubMed]
110. Akkus, Z.B.; Nazir, I.; Jalil, A.; Tribus, M.; Bernkop-Schnürch, A. Zeta Potential Changing Polyphosphate Nanoparticles: A Promising Approach To Overcome the Mucus and Epithelial Barrier. *Mol. Pharm.* **2019**, *16*, 2817–2825. [CrossRef]
111. Li, H.-J.; Du, J.-Z.; Du, X.-J.; Xu, C.-F.; Sun, C.-Y.; Wang, H.-X.; Cao, Z.-T.; Yang, X.-Z.; Zhu, Y.-H.; Nie, S.; et al. Stimuli-Responsive Clustered Nanoparticles for Improved Tumor Penetration and Therapeutic Efficacy. *Proc. Natl. Acad. Sci. USA* **2016**, *113*, 4164–4169. [CrossRef]
112. Radovic-Moreno, A.F.; Lu, T.K.; Puscasu, V.A.; Yoon, C.J.; Langer, R.; Farokhzad, O.C. Surface Charge-Switching Polymeric Nanoparticles for Bacterial Cell Wall-Targeted Delivery of Antibiotics. *ACS Nano* **2012**, *6*, 4279–4287. [CrossRef]
113. Zhou, Q.; Hou, Y.; Zhang, L.; Wang, J.; Qiao, Y.; Guo, S.; Fan, L.; Yang, T.; Zhu, L.; Wu, H. Dual-pH Sensitive Charge-Reversal Nanocomplex for Tumor-Targeted Drug Delivery with Enhanced Anticancer Activity. *Theranostics* **2017**, *7*, 1806–1819. [CrossRef]
114. Behbahani, S.B.; Kiridena, S.D.; Wijayaratna, U.N.; Taylor, C.; Anker, J.N.; Tzeng, T.-R.J. pH Variation in Medical Implant Biofilms: Causes, Measurements, and Its Implications for Antibiotic Resistance. *Front. Microbiol.* **2022**, *13*, 1028560. [CrossRef]
115. Andreucci, E.; Peppicelli, S.; Ruzzolini, J.; Bianchini, F.; Biagioni, A.; Papucci, L.; Magnelli, L.; Mazzanti, B.; Stecca, B.; Calorini, L. The Acidic Tumor Microenvironment Drives a Stem-like Phenotype in Melanoma Cells. *J. Mol. Med.* **2020**, *98*, 1431–1446. [CrossRef]
116. Merkl, P.; Aschtgen, M.-S.; Henriques-Normark, B.; Sotiriou, G.A. Biofilm Interfacial Acidity Evaluation by pH-Responsive Luminescent Nanoparticle Films. *Biosens. Bioelectron.* **2021**, *171*, 112732. [CrossRef] [PubMed]

117. Hollmann, B.; Perkins, M.; Chauhan, V.M.; Aylott, J.W.; Hardie, K.R. Fluorescent Nanosensors Reveal Dynamic pH Gradients during Biofilm Formation. *npj Biofilms Microbiomes* **2021**, *7*, 50. [CrossRef]
118. Chinapaka, R.; Sivaramakrishna, D.; Choudhury, S.K.; Manasa, K.; Cheppali, S.K.; Swamy, M.J. Structure, Self-Assembly, and Phase Behavior of Neuroactive N-Acyl GABAs: Doxorubicin Encapsulation in NPGABA/DPPC Liposomes and Release Studies. *Langmuir* **2024**, *40*, 7883–7895. [CrossRef]
119. Yang, C.; Liu, P. Disulfide/α-Amide-Bridged Doxorubicin Dimeric Prodrug: Effect of Aggregation Structures on pH/GSH Dual-Triggered Drug Release. *Langmuir* **2024**, *40*, 11098–11105. [CrossRef] [PubMed]
120. Basutkar, N.B.; Surapaneni, S.G.; Alam, M.S.; Ambade, A.V. Visible Light and pH-Responsive Star Copolymer and Doxorubicin-Polymer Conjugate Micelles for Combination Drug Delivery and Bioimaging. *J. Macromol. Sci. Part A* **2024**, *61*, 105–116. [CrossRef]
121. Aram, E.; Sadeghi-Abandansari, H.; Radmanesh, F.; Khorasani, H.R.; Nowroozi, M.R.; Hassanpour, A.; Baharvand, H.; Sabour, D. Shell-Sheddable and Charge Switchable Magnetic Nanoparticle as pH-Sensitive Nanocarrier for Targeted Drug Delivery Applications. *Polym. Adv. Technol.* **2024**, *35*, e6366. [CrossRef]
122. Qiao, Z.; Yao, Y.; Song, S.; Yin, M.; Luo, J. Silver Nanoparticles with pH Induced Surface Charge Switchable Properties for Antibacterial and Antibiofilm Applications. *J. Mater. Chem. B* **2019**, *7*, 830–840. [CrossRef]
123. Xing, F.; Hu, Q.; Qin, Y.; Xu, J.; Zhang, B.; Yu, X.; Wang, W. The Relationship of Redox With Hallmarks of Cancer: The Importance of Homeostasis and Context. *Front. Oncol.* **2022**, *12*, 862743. [CrossRef]
124. Ranbhise, J.S.; Singh, M.K.; Ju, S.; Han, S.; Yun, H.R.; Kim, S.S.; Kang, I. The Redox Paradox: Cancer's Double-Edged Sword for Malignancy and Therapy. *Antioxidants* **2025**, *14*, 1187. [CrossRef]
125. Abed, H.F.; Abuwatfa, W.H.; Husseini, G.A. Redox-Responsive Drug Delivery Systems: A Chemical Perspective. *Nanomaterials* **2022**, *12*, 3183. [CrossRef]
126. Jia, L.; Li, Z.; Zheng, D.; Li, Z.; Zhao, Z. A Targeted and Redox/pH-Responsive Chitosan Oligosaccharide Derivatives Based Nanohybrids for Overcoming Multidrug Resistance of Breast Cancer Cells. *Carbohydr. Polym.* **2021**, *251*, 117008. [CrossRef] [PubMed]
127. Sauraj; Kumar, V.; Kumar, B.; Priyadarshi, R.; Deeba, F.; Kulshreshtha, A.; Kumar, A.; Agrawal, G.; Gopinath, P.; Negi, Y.S. Redox Responsive Xylan-SS-Curcumin Prodrug Nanoparticles for Dual Drug Delivery in Cancer Therapy. *Mater. Sci. Eng. C* **2020**, *107*, 110356. [CrossRef]
128. Zhang, Y.; Zhou, J.; Yang, C.; Wang, W.; Chu, L.; Huang, F.; Liu, Q.; Deng, L.; Kong, D.; Liu, J.; et al. Folic Acid-Targeted Disulfide-Based Cross-Linking Micelle for Enhanced Drug Encapsulation Stability and Site-Specific Drug Delivery Against Tumors [Corrigendum]. *Int. J. Nanomed.* **2021**, *16*, 7683–7684. [CrossRef] [PubMed]
129. Du, Z.; Saleh, E.A.M.; Moharam, M.M.; Rab, S.O.; Ballal, S.; Singh, A.; Sabarivani, A.; Sahoo, S.; Hsu, C.-Y. Enzyme Responsive Magnetic Nanoparticles for Targeted Drug Delivery and Precision Medicine. *Drug Dev. Res.* **2025**, *86*, e70185. [CrossRef]
130. Sullivan, H.L.; Liang, Y.; Worthington, K.; Luo, C.; Gianneschi, N.C.; Christman, K.L. Enzyme-Responsive Nanoparticles for the Targeted Delivery of an MMP Inhibitor to Acute Myocardial Infarction. *Biomacromolecules* **2023**, *24*, 4695–4704. [CrossRef] [PubMed]
131. Hao, X.; Zhang, H.; Yang, Y.; Lin, Z.; Bao, H.; Huang, X.; Yao, G.; Yang, Q.; Qian, J.; Zhang, Y. Enzyme-Responsive Biomimetic Ferritin Nanoparticles for Selective Cancer Therapy. *Biomaterials* **2026**, *325*, 123545. [CrossRef]
132. Grützner, V.; Unger, R.E.; Baier, G.; Choritz, L.; Freese, C.; Böse, T.; Landfester, K.; Kirkpatrick, C.J. Enzyme-Responsive Nanocomposites for Wound Infection Prophylaxis in Burn Management: In Vitro Evaluation of Their Compatibility with Healing Processes. *Int. J. Nanomed.* **2015**, *10*, 4111–4124. [CrossRef] [PubMed]
133. Li, W.; Li, Y.; Liu, Z.; Kerdsakundee, N.; Zhang, M.; Zhang, F.; Liu, X.; Bauleth-Ramos, T.; Lian, W.; Mäkilä, E.; et al. Hierarchical Structured and Programmed Vehicles Deliver Drugs Locally to Inflamed Sites of Intestine. *Biomaterials* **2018**, *185*, 322–332. [CrossRef] [PubMed]
134. Farjadian, F.; Ghasemi, S.; Akbarian, M.; Hoseini-Ghahfarokhi, M.; Moghoofei, M.; Doroudian, M. Physically Stimulus-Responsive Nanoparticles for Therapy and Diagnosis. *Front. Chem.* **2022**, *10*, 952675. [CrossRef]
135. Han, M.; Yildiz, E.; Bozuyuk, U.; Aydin, A.; Yu, Y.; Bhargava, A.; Karaz, S.; Sitti, M. Janus Microparticles-Based Targeted and Spatially-Controlled Piezoelectric Neural Stimulation via Low-Intensity Focused Ultrasound. *Nat. Commun.* **2024**, *15*, 2013. [CrossRef]
136. Tharkar, P.; Varanasi, R.; Wong, W.S.F.; Jin, C.T.; Chrzanowski, W. Nano-Enhanced Drug Delivery and Therapeutic Ultrasound for Cancer Treatment and Beyond. *Front. Bioeng. Biotechnol.* **2019**, *7*, 324. [CrossRef] [PubMed]
137. Nunziata, G.; Nava, M.; Lacroce, E.; Pizzetti, F.; Rossi, F. Thermo-Responsive Polymer-Based Nanoparticles: From Chemical Design to Advanced Applications. *Macromol. Rapid Commun.* **2025**, *46*, 2401127. [CrossRef]
138. Wang, X.; Li, C.; Wang, Y.; Chen, H.; Zhang, X.; Luo, C.; Zhou, W.; Li, L.; Teng, L.; Yu, H.; et al. Smart Drug Delivery Systems for Precise Cancer Therapy. *Acta Pharm. Sin. B* **2022**, *12*, 4098–4121. [CrossRef] [PubMed]

139. Ribeiro, T.P.; Gomes, F.L.; Vilarinho, R.; Salgado, C.; Martins, M.C.L.; Moreira, J.A.; Monteiro, F.J.; Laranjeira, M.S. Thermoresponsive Nanoparticles for Targeted and Controlled Delivery of Doxorubicin in Triple Negative Breast Cancer: A 2D and 3D in Vitro Evaluation. *Drug Deliv. Transl. Res.* **2026**, *16*, 108–123. [CrossRef]
140. Wang, T.; Wu, C.; Hu, Y.; Zhang, Y.; Ma, J. Stimuli-Responsive Nanocarrier Delivery Systems for Pt-Based Antitumor Complexes: A Review. *RSC Adv.* **2023**, *13*, 16488–16511. [CrossRef]
141. Wang, L.; Zhang, J.; An, Y.; Wang, Z.; Liu, J.; Li, Y.; Zhang, D. A Study on the Thermochemotherapy Effect of Nanosized As_2O_3/MZF Thermosensitive Magnetoliposomes on Experimental Hepatoma in Vitro and in Vivo. *Nanotechnology* **2011**, *22*, 315102. [CrossRef] [PubMed]
142. Li, Z.; Li, X.; Lu, Y.; Zhu, X.; Zheng, W.; Chen, K.; Liu, S.; Wu, J.; Guan, W. Improved Photodynamic Therapy Based on Glutaminase Blockage via Tumor Membrane Coated CB-839/IR-780 Nanoparticles. *Small* **2024**, *20*, 2305174. [CrossRef]
143. Sánchez-Moreno, P.; de Vicente, J.; Nardecchia, S.; Marchal, J.A.; Boulaiz, H. Thermo-Sensitive Nanomaterials: Recent Advance in Synthesis and Biomedical Applications. *Nanomaterials* **2018**, *8*, 935. [CrossRef]
144. Xiang, J.; Tong, X.; Shi, F.; Yan, Q.; Yu, B.; Zhao, Y. Near-Infrared Light-Triggered Drug Release from UV-Responsive Diblock Copolymer-Coated Upconversion Nanoparticles with High Monodispersity. *J. Mater. Chem. B* **2018**, *6*, 3531–3540. [CrossRef]
145. Han, J.; Zhang, Y.; Wang, X.; Zhang, G.; Yu, Z.; Wang, C.; Xu, T.; Zhou, Z.; Yang, X.; Jin, X.; et al. Ultrasound-Mediated Piezoelectric Nanoparticle Modulation of Intrinsic Cardiac Autonomic Nervous System for Rate Control in Atrial Fibrillation. *Biomater. Sci.* **2023**, *11*, 655–665. [CrossRef]
146. Liu, D.; Yang, F.; Xiong, F.; Gu, N. The Smart Drug Delivery System and Its Clinical Potential. *Theranostics* **2016**, *6*, 1306–1323. [CrossRef]
147. Chen, Z.; Sang, L.; Qixi, Z.; Li, X.; Liu, Y.; Bai, Z. Ultrasound-Responsive Nanoparticles for Imaging and Therapy of Brain Tumors. *Mater. Today Bio* **2025**, *32*, 101661. [CrossRef] [PubMed]
148. Wang, M.; Yang, Q.; Li, M.; Zou, H.; Wang, Z.; Ran, H.; Zheng, Y.; Jian, J.; Zhou, Y.; Luo, Y.; et al. Multifunctional Nanoparticles for Multimodal Imaging-Guided Low-Intensity Focused Ultrasound/Immunosynergistic Retinoblastoma Therapy. *ACS Appl. Mater. Interfaces* **2020**, *12*, 5642–5657. [CrossRef]
149. Deng, X.; Liu, X.; Zhao, L. Multifunctional Nanoplatforms for Tumor Microenvironment Remodeling: Toward Precision and Intelligent Cancer Therapy. *Mater. Today Bio* **2025**, *35*, 102385. [CrossRef] [PubMed]
150. Chen, Y.; Ma, H.; Wang, W.; Zhang, M. A Size-Tunable Nanoplatform: Enhanced MMP2-Activated Chemo-Photodynamic Immunotherapy Based on Biodegradable Mesoporous Silica Nanoparticles. *Biomater. Sci.* **2021**, *9*, 917–929. [CrossRef] [PubMed]
151. Sun, L.; Xie, S.; Qi, J.; Liu, E.; Liu, D.; Liu, Q.; Chen, S.; He, H.; Yang, V.C. Cell-Permeable, MMP-2 Activatable, Nickel Ferrite and His-Tagged Fusion Protein Self-Assembled Fluorescent Nanoprobe for Tumor Magnetic-Targeting and Imaging. *ACS Appl. Mater. Interfaces* **2017**, *9*, 39209–39222. [CrossRef] [PubMed]
152. Fan, R.; Chen, C.; Mu, M.; Chuan, D.; Liu, H.; Hou, H.; Huang, J.; Tong, A.; Guo, G.; Xu, J. Engineering MMP-2 Activated Nanoparticles Carrying B7-H3 Bispecific Antibodies for Ferroptosis-Enhanced Glioblastoma Immunotherapy. *ACS Nano* **2023**, *17*, 9126–9139. [CrossRef]
153. Yang, Y.; Sun, W. Recent Advances in Redox-Responsive Nanoparticles for Combined Cancer Therapy. *Nanoscale Adv.* **2022**, *4*, 3504–3516. [CrossRef]
154. Sun, C.; Li, X.; Du, X.; Wang, T. Redox-Responsive Micelles for Triggered Drug Delivery and Effective Laryngopharyngeal Cancer Therapy. *Int. J. Biol. Macromol.* **2018**, *112*, 65–73. [CrossRef] [PubMed]
155. Dong, Y.; Li, J.; Dai, Y.; Zhang, X.; Wang, T.; Zhao, B.; Liu, W.; Chen, L.; Yang, S.; Du, P.; et al. Redox-Responsive Metal-Organic Framework Nanocapsules Enhance Tumor Chemo-Immunotherapy by Modulating Tumor Metabolic Reprogramming. *Mater. Today Bio* **2025**, *31*, 101487. [CrossRef]
156. Lu, H.; Xu, S.; Guo, Z.; Zhao, M.; Liu, Z. Redox-Responsive Molecularly Imprinted Nanoparticles for Targeted Intracellular Delivery of Protein toward Cancer Therapy. *ACS Nano* **2021**, *15*, 18214–18225. [CrossRef] [PubMed]
157. Badparvar, F.; Marjani, A.P.; Salehi, R.; Ramezani, F. Dual pH/Redox-Responsive Hyperbranched Polymeric Nanocarriers with TME-Trigger Size Shrinkage and Charge Reversible Ability for Amplified Chemotherapy of Breast Cancer. *Sci. Rep.* **2024**, *14*, 8567. [CrossRef]
158. Wang, W.; Yao, S.-Y.; Luo, J.; Ding, C.; Huang, Q.; Yang, Y.; Shi, Z.; Lin, J.; Pan, Y.-C.; Zeng, X.; et al. Engineered Hypoxia-Responsive Albumin Nanoparticles Mediating Mitophagy Regulation for Cancer Therapy. *Nat. Commun.* **2025**, *16*, 596. [CrossRef]
159. Zhang, P.; Yang, H.; Shen, W.; Liu, W.; Chen, L.; Xiao, C. Hypoxia-Responsive Polypeptide Nanoparticles Loaded with Doxorubicin for Breast Cancer Therapy. *ACS Biomater. Sci. Eng.* **2020**, *6*, 2167–2174. [CrossRef]
160. AlQurashi, D.M.; AlQurashi, T.F.; Alam, R.I.; Shaikh, S.; Tarkistani, M.A.M. Advanced Nanoparticles in Combating Antibiotic Resistance: Current Innovations and Future Directions. *J. Nanotheranostics* **2025**, *6*, 9. [CrossRef]
161. Qing, Y.; Cheng, L.; Li, R.; Liu, G.; Zhang, Y.; Tang, X.; Wang, J.; Liu, H.; Qin, Y. Potential Antibacterial Mechanism of Silver Nanoparticles and the Optimization of Orthopedic Implants by Advanced Modification Technologies. *Int. J. Nanomed.* **2018**, *13*, 3311–3327. [CrossRef]

162. Dakal, T.C.; Kumar, A.; Majumdar, R.S.; Yadav, V. Mechanistic Basis of Antimicrobial Actions of Silver Nanoparticles. *Front. Microbiol.* **2016**, *7*, 1831. [CrossRef]
163. Normani, S.; Dalla Vedova, N.; Lanzani, G.; Scotognella, F.; Paternò, G.M. Bringing the Interaction of Silver Nanoparticles with Bacteria to Light. *Biophys. Rev.* **2021**, *2*, 021304. [CrossRef]
164. Rukavina, Z.; Vanić, Ž. Current Trends in Development of Liposomes for Targeting Bacterial Biofilms. *Pharmaceutics* **2016**, *8*, 18. [CrossRef]
165. Makhlouf, Z.; Ali, A.A.; Al-Sayah, M.H. Liposomes-Based Drug Delivery Systems of Anti-Biofilm Agents to Combat Bacterial Biofilm Formation. *Antibiotics* **2023**, *12*, 875. [CrossRef] [PubMed]
166. Scheeder, A.; Brockhoff, M.; Ward, E.N.; Kaminski Schierle, G.S.; Mela, I.; Kaminski, C.F. Molecular Mechanisms of Cationic Fusogenic Liposome Interactions with Bacterial Envelopes. *J. Am. Chem. Soc.* **2023**, *145*, 28240–28250. [CrossRef]
167. Lu, P.; Zhang, X.; Li, F.; Xu, K.-F.; Li, Y.-H.; Liu, X.; Yang, J.; Zhu, B.; Wu, F.-G. Cationic Liposomes with Different Lipid Ratios: Antibacterial Activity, Antibacterial Mechanism, and Cytotoxicity Evaluations. *Pharmaceuticals* **2022**, *15*, 1556. [CrossRef]
168. Guo, R.; Liu, Y.; Li, K.; Tian, B.; Li, W.; Niu, S.; Hong, W. Direct Interactions between Cationic Liposomes and Bacterial Cells Ameliorate the Systemic Treatment of Invasive Multidrug-Resistant *Staphylococcus aureus* Infections. *Nanomed. Nanotechnol. Biol. Med.* **2021**, *34*, 102382. [CrossRef] [PubMed]
169. Deiss-Yehiely, E.; Cárcamo-Oyarce, G.; Berger, A.G.; Ribbeck, K.; Hammond, P.T. pH-Responsive, Charge-Reversing Layer-by-Layer Nanoparticle Surfaces Enhance Biofilm Penetration and Eradication. *ACS Biomater. Sci. Eng.* **2023**, *9*, 4794–4804. [CrossRef]
170. Jiang, Y.; Zheng, W.; Tran, K.; Ma, H.; Liang, H. Transformation from Hydrophilic Yet Membrane-Inactive Linear Chain Polymers to Membrane-Active Nanoantibiotics. *Biomacromolecules* **2025**, *26*, 4690–4701. [CrossRef] [PubMed]
171. Jiang, Y.; Zheng, W.; Tran, K.; Kamilar, E.; Bariwal, J.; Ma, H.; Liang, H. Hydrophilic Nanoparticles That Kill Bacteria While Sparing Mammalian Cells Reveal the Antibiotic Role of Nanostructures. *Nat. Commun.* **2022**, *13*, 197. [CrossRef] [PubMed]
172. You, Y.; Yu, X.; Jiang, J.; Chen, Z.; Zhu, Y.-X.; Chen, Y.; Lin, H.; Shi, J. Bacterial Cell Wall-Specific Nanomedicine for the Elimination of Staphylococcus Aureus and Pseudomonas Aeruginosa Through Electron-Mechanical Intervention. *Nat. Commun.* **2025**, *16*, 2836. [CrossRef]
173. Alavi, M.; Kamarasu, P.; McClements, D.J.; Moore, M.D. Metal and Metal Oxide-Based Antiviral Nanoparticles: Properties, Mechanisms of Action, and Applications. *Adv. Colloid Interface Sci.* **2022**, *306*, 102726. [CrossRef] [PubMed]
174. Huang, Y.; Guo, X.; Wu, Y.; Chen, X.; Feng, L.; Xie, N.; Shen, G. Nanotechnology's Frontier in Combatting Infectious and Inflammatory Diseases: Prevention and Treatment. *Signal Transduct. Target. Ther.* **2024**, *9*, 34. [CrossRef] [PubMed]
175. Trigilio, J.; Antoine, T.E.; Paulowicz, I.; Mishra, Y.K.; Adelung, R.; Shukla, D. Tin Oxide Nanowires Suppress Herpes Simplex Virus-1 Entry and Cell-to-Cell Membrane Fusion. *PLoS ONE* **2012**, *7*, e48147. [CrossRef]
176. Meléndez-Villanueva, M.A.; Morán-Santibañez, K.; Martínez-Sanmiguel, J.J.; Rangel-López, R.; Garza-Navarro, M.A.; Rodríguez-Padilla, C.; Zarate-Triviño, D.G.; Trejo-Ávila, L.M. Virucidal Activity of Gold Nanoparticles Synthesized by Green Chemistry Using Garlic Extract. *Viruses* **2019**, *11*, 1111. [CrossRef]
177. Kong, B.; Moon, S.; Kim, Y.; Heo, P.; Jung, Y.; Yu, S.-H.; Chung, J.; Ban, C.; Kim, Y.H.; Kim, P.; et al. Virucidal Nano-Perforator of Viral Membrane Trapping Viral RNAs in the Endosome. *Nat. Commun.* **2019**, *10*, 185. [CrossRef]
178. Sun, Y.; Gong, L.; Yin, Y.; Zhang, L.; Sun, Q.; Feng, K.; Cui, Y.; Zhang, Q.; Zhang, X.; Deng, X.; et al. A Gradient pH-Sensitive Polymer-Based Antiviral Strategy via Viroporin-Induced Membrane Acidification. *Adv. Mater.* **2022**, *34*, 2109580. [CrossRef]
179. Kim, J.; Yeom, M.; Lee, T.; Kim, H.-O.; Na, W.; Kang, A.; Lim, J.-W.; Park, G.; Park, C.; Song, D.; et al. Porous Gold Nanoparticles for Attenuating Infectivity of Influenza A Virus. *J. Nanobiotechnol.* **2020**, *18*, 54. [CrossRef]
180. Jeremiah, S.S.; Miyakawa, K.; Morita, T.; Yamaoka, Y.; Ryo, A. Potent Antiviral Effect of Silver Nanoparticles on SARS-CoV-2. *Biochem. Biophys. Res. Commun.* **2020**, *533*, 195–200. [CrossRef]
181. Rios-Ibarra, C.P.; Salinas-Santander, M.; Orozco-Nunnelly, D.A.; Bravo-Madrigal, J. Nanoparticle-based Antiviral Strategies to Combat the Influenza Virus (Review). *Biomed. Rep.* **2024**, *20*, 65. [CrossRef]
182. Antoine, T.E.; Hadigal, S.R.; Yakoub, A.M.; Mishra, Y.K.; Bhattacharya, P.; Haddad, C.; Valyi-Nagy, T.; Adelung, R.; Prabhakar, B.S.; Shukla, D. Intravaginal Zinc Oxide Tetrapod Nanoparticles as Novel Immunoprotective Agents against Genital Herpes. *J. Immunol.* **2016**, *196*, 4566–4575. [CrossRef]
183. Warnes, S.L.; Little, Z.R.; Keevil, C.W. Human Coronavirus 229E Remains Infectious on Common Touch Surface Materials. *mBio* **2015**, *6*, 10–1128. [CrossRef]
184. Park, G.W.; Cho, M.; Cates, E.L.; Lee, D.; Oh, B.-T.; Vinjé, J.; Kim, J.-H. Fluorinated TiO_2 as an Ambient Light-Activated Virucidal Surface Coating Material for the Control of Human Norovirus. *J. Photochem. Photobiol. B* **2014**, *140*, 315–320. [CrossRef] [PubMed]
185. Duong, N.L.; Nguyen, V.M.; Tran, T.A.N.; Phan, T.D.T.; Tran, T.B.Y.; Do, B.L.; Phung Anh, N.; Nguyen, T.A.T.; Ho, T.G.-T.; Nguyen, T. Durian Shell-Mediated Simple Green Synthesis of Nanocopper against Plant Pathogenic Fungi. *ACS Omega* **2023**, *8*, 10968–10979. [CrossRef]

186. Azadi, S.; Azizipour, E.; Amani, A.M.; Vaez, A.; Zareshahrabadi, Z.; Abbaspour, A.; Firuzyar, T.; Dortaj, H.; Kamyab, H.; Chelliapan, S.; et al. Antifungal Activity of Fe_3O_4@SiO_2/Schiff-Base/Cu(II) Magnetic Nanoparticles against Pathogenic Candida Species. *Sci. Rep.* **2024**, *14*, 5855. [CrossRef]
187. Saritha, C.; Rajana, V.K.; Choudhary, K.; Vairagar, A.; Mishra, A.; Penumaka, S.M.; Jain, S.; Dande, A.; Naresh, P.; Kumar, N.; et al. Highly Selective Ergosterol Binding and Impaired Redox Balance Leads to Improved Antileishmanial Efficacy for Amphotericin b Synthesized Silver Nanoparticles with Reduced Toxicity– In Vitro and in Vivo Studies. *Free Radic. Biol. Med.* **2025**, *235*, 405–425. [CrossRef] [PubMed]
188. Kischkel, B.; Rossi, S.A.; Santos, S.R.; Nosanchuk, J.D.; Travassos, L.R.; Taborda, C.P. Therapies and Vaccines Based on Nanoparticles for the Treatment of Systemic Fungal Infections. *Front. Cell. Infect. Microbiol.* **2020**, *10*, 463. [CrossRef]
189. Radwan, M.A.; AlQuadeib, B.T.; Šiller, L.; Wright, M.C.; Horrocks, B. Oral Administration of Amphotericin B Nanoparticles: Antifungal Activity, Bioavailability and Toxicity in Rats. *Drug Deliv.* **2017**, *24*, 40–50. [CrossRef] [PubMed]
190. Chen, Q.; Yu, T.; Gong, J.; Shan, H. Advanced Nanomedicine Delivery Systems for Cardiovascular Diseases: Viral and Non-Viral Strategies in Targeted Therapy. *Molecules* **2025**, *30*, 962. [CrossRef]
191. Guo, T.; Chen, L.; Li, F.; Cao, Y.; Li, D.; Xiong, Q.; Ling, Z. Biomimetic Nanoparticles Loaded Lutein Functionalized by Macrophage Membrane for Targeted Amelioration Pressure Overload-Induced Cardiac Fibrosis. *Biomed. Pharmacother.* **2023**, *167*, 115579. [CrossRef]
192. Wu, Y.; Wan, S.; Yang, S.; Hu, H.; Zhang, C.; Lai, J.; Zhou, J.; Chen, W.; Tang, X.; Luo, J.; et al. Macrophage Cell Membrane-Based Nanoparticles: A New Promising Biomimetic Platform for Targeted Delivery and Treatment. *J. Nanobiotechnol.* **2022**, *20*, 542. [CrossRef]
193. Kim, K.; Park, S.; Park, J.; Choi, J.-H. Characteristics of Plaque Lipid-Associated Macrophages and Their Possible Roles in the Pathogenesis of Atherosclerosis. *Curr. Opin. Lipidol.* **2022**, *33*, 283–288. [CrossRef] [PubMed]
194. Swirski, F.K.; Libby, P.; Aikawa, E.; Alcaide, P.; Luscinskas, F.W.; Weissleder, R.; Pittet, M.J. Ly-6C^{hi} Monocytes Dominate Hypercholesterolemia-Associated Monocytosis and Give Rise to Macrophages in Atheromata. *J. Clin. Investig.* **2007**, *117*, 195–205. [CrossRef] [PubMed]
195. Gifani, M.; Eddins, D.J.; Kosuge, H.; Zhang, Y.; Paluri, S.L.A.; Larson, T.; Leeper, N.; Herzenberg, L.A.; Gambhir, S.S.; McConnell, M.V.; et al. Ultra-Selective Carbon Nanotubes for Photoacoustic Imaging of Inflamed Atherosclerotic Plaques. *Adv. Funct. Mater.* **2021**, *31*, 2101005. [CrossRef]
196. Chai, A.B.; Callaghan, R.; Gelissen, I.C. Regulation of P-Glycoprotein in the Brain. *Int. J. Mol. Sci.* **2022**, *23*, 14667. [CrossRef] [PubMed]
197. Wang, C.; Xue, Y.; Markovic, T.; Li, H.; Wang, S.; Zhong, Y.; Du, S.; Zhang, Y.; Hou, X.; Yu, Y.; et al. Blood–Brain-Barrier-Crossing Lipid Nanoparticles for mRNA Delivery to the Central Nervous System. *Nat. Mater.* **2025**, *24*, 1653–1663. [CrossRef]
198. Writing Committee for the HEALEY ALS Platform Trial; HEALEY ALS Platform Trial Study Group. CNM-Au8 in Amyotrophic Lateral Sclerosis: The HEALEY ALS Platform Trial. *JAMA* **2025**, *333*, 1138–1149. [CrossRef]
199. Wang, Z.; Henriques, A.; Rouvière, L.; Callizot, N.; Tan, L.; Hotchkin, M.T.; Rossignol, R.; Mortenson, M.G.; Dorfman, A.R.; Ho, K.S.; et al. A Mechanism Underpinning the Bioenergetic Metabolism-Regulating Function of Gold Nanocatalysts. *Small* **2024**, *20*, 2304082. [CrossRef]
200. Alqahtani, T.; Deore, S.L.; Kide, A.A.; Shende, B.A.; Sharma, R.; Dadarao Chakole, R.; Nemade, L.S.; Kishor Kale, N.; Borah, S.; Shrikant Deokar, S.; et al. Mitochondrial Dysfunction and Oxidative Stress in Alzheimer's Disease, and Parkinson's Disease, Huntington's Disease and Amyotrophic Lateral Sclerosis -An Updated Review. *Mitochondrion* **2023**, *71*, 83–92. [CrossRef]
201. Yang, W.; Zhang, M.; He, J.; Gong, M.; Sun, J.; Yang, X. Central Nervous System Injury Meets Nanoceria: Opportunities and Challenges. *Regen. Biomater.* **2022**, *9*, rbac037. [CrossRef]
202. Sun, H.; Li, Y.; Xue, M.; Feng, D. Tumor Microenvironment-Responsive Nanoparticles: Promising Cancer PTT Carriers. *Int. J. Nanomed.* **2025**, *20*, 7987–8001. [CrossRef]
203. Thomas, R.G.; Surendran, S.P.; Jeong, Y.Y. Tumor Microenvironment-Stimuli Responsive Nanoparticles for Anticancer Therapy. *Front. Mol. Biosci.* **2020**, *7*, 610533. [CrossRef] [PubMed]
204. Lin, H.-H.; Lin, H.-K.; Lin, I.-H.; Chiou, Y.-W.; Chen, H.-W.; Liu, C.-Y.; Harn, H.I.-C.; Chiu, W.-T.; Wang, Y.-K.; Shen, M.-R.; et al. Mechanical Phenotype of Cancer Cells: Cell Softening and Loss of Stiffness Sensing. *Oncotarget* **2015**, *6*, 20946–20958. [CrossRef]
205. Alibert, C.; Goud, B.; Manneville, J.-B. Are Cancer Cells Really Softer than Normal Cells? *Biol. Cell* **2017**, *109*, 167–189. [CrossRef] [PubMed]
206. Desai, N.; Rana, D.; Pande, S.; Salave, S.; Giri, J.; Benival, D.; Kommineni, N. "Bioinspired" Membrane-Coated Nanosystems in Cancer Theranostics: A Comprehensive Review. *Pharmaceutics* **2023**, *15*, 1677. [CrossRef]
207. Fatima, R.; Katiyar, P.; Kushwaha, K. Recent Advances in Mesoporous Silica Nanoparticle: Synthesis, Drug Loading, Release Mechanisms, and Diverse Applications. *Front. Nanotechnol.* **2025**, *7*, 1564188. [CrossRef]

208. Ahmadi, F.; Sodagar-Taleghani, A.; Ebrahimnejad, P.; Pouya Hadipour Moghaddam, S.; Ebrahimnejad, F.; Asare-Addo, K.; Nokhodchi, A. A Review on the Latest Developments of Mesoporous Silica Nanoparticles as a Promising Platform for Diagnosis and Treatment of Cancer. *Int. J. Pharm.* **2022**, *625*, 122099. [CrossRef]
209. Kumar, P.; Tambe, P.; Paknikar, K.M.; Gajbhiye, V. Mesoporous Silica Nanoparticles as Cutting-Edge Theranostics: Advancement from Merely a Carrier to Tailor-Made Smart Delivery Platform. *J. Control. Release* **2018**, *287*, 35–57. [CrossRef]
210. Miao, Y.; Bao, Q.; Yang, T.; Yang, M.; Mao, C. Magnetic Multifunctional Nanoparticles for Effective Targeted Cancer Therapy. *Adv. NanoBiomed Res.* **2025**, *5*, 2400176. [CrossRef]
211. Chen, W.-H.; Luo, G.-F.; Lei, Q.; Cao, F.-Y.; Fan, J.-X.; Qiu, W.-X.; Jia, H.-Z.; Hong, S.; Fang, F.; Zeng, X.; et al. Rational Design of Multifunctional Magnetic Mesoporous Silica Nanoparticle for Tumor-Targeted Magnetic Resonance Imaging and Precise Therapy. *Biomaterials* **2016**, *76*, 87–101. [CrossRef] [PubMed]
212. Bui, L.; Edwards, S.; Hall, E.; Alderfer, L.; Round, K.; Owen, M.; Sainaghi, P.; Zhang, S.; Nallathamby, P.D.; Haneline, L.S.; et al. Engineering Bioactive Nanoparticles to Rejuvenate Vascular Progenitor Cells. *Commun. Biol.* **2022**, *5*, 635. [CrossRef] [PubMed]
213. Ba, S.; Qiao, M.; Jia, L.; Zhang, J.; Zhao, X.; Hu, H.; Chen, D. Construction of Hierarchical-Targeting pH-Sensitive Liposomes to Reverse Chemotherapeutic Resistance of Cancer Stem-like Cells. *Pharmaceutics* **2021**, *13*, 1205. [CrossRef]
214. Nair, L.V.; Nazeer, S.S.; Jayasree, R.S.; Ajayaghosh, A. Fluorescence Imaging Assisted Photodynamic Therapy Using Photosensitizer-Linked Gold Quantum Clusters. *ACS Nano* **2015**, *9*, 5825–5832. [CrossRef]
215. Boada, C.A.; Zinger, A.; Rohen, S.; Martinez, J.O.; Evangelopoulos, M.; Molinaro, R.; Lu, M.; Villarreal-Leal, R.A.; Giordano, F.; Sushnitha, M.; et al. LDL-Based Lipid Nanoparticle Derived for Blood Plasma Accumulates Preferentially in Atherosclerotic Plaque. *Front. Bioeng. Biotechnol.* **2021**, *9*, 794676. [CrossRef] [PubMed]
216. Chen, X.; Chen, F.-Y.; Lu, Y.; Li, Q.; Li, S.; Zheng, C.; Zheng, Y.; Dang, L.; Li, R.-Y.; Liu, Y.; et al. Supramolecular Nano-Tracker for Real-Time Tracking of Drug Release and Efficient Combination Therapy. *Adv. Sci.* **2024**, *11*, 2404731. [CrossRef]
217. Rahman, M. Magnetic Resonance Imaging and Iron-Oxide Nanoparticles in the Era of Personalized Medicine. *Nanotheranostics* **2023**, *7*, 424–449. [CrossRef]
218. Al-Jamal, K.T.; Bai, J.; Wang, J.T.-W.; Protti, A.; Southern, P.; Bogart, L.; Heidari, H.; Li, X.; Cakebread, A.; Asker, D.; et al. Magnetic Drug Targeting: Preclinical in Vivo Studies, Mathematical Modeling, and Extrapolation to Humans. *Nano Lett.* **2016**, *16*, 5652–5660. [CrossRef]
219. Lin, L.-S.; Song, J.; Song, L.; Ke, K.; Liu, Y.; Zhou, Z.; Shen, Z.; Li, J.; Yang, Z.; Tang, W.; et al. Simultaneous Fenton-like Ion Delivery and Glutathione Depletion by MnO_2-Based Nanoagent to Enhance Chemodynamic Therapy. *Angew. Chem. Int. Ed.* **2018**, *57*, 4902–4906. [CrossRef]
220. Cole, L.E.; McGinnity, T.L.; Irimata, L.E.; Vargo-Gogola, T.; Roeder, R.K. Effects of Bisphosphonate Ligands and PEGylation on Targeted Delivery of Gold Nanoparticles for Contrast-Enhanced Radiographic Detection of Breast Microcalcifications. *Acta Biomater.* **2018**, *82*, 122–132. [CrossRef]
221. McGinnity, T.L.; Dominguez, O.; Curtis, T.E.; Nallathamby, P.D.; Hoffman, A.J.; Roeder, R.K. Hafnia (HfO_2) Nanoparticles as an X-Ray Contrast Agent and Mid-Infrared Biosensor. *Nanoscale* **2016**, *8*, 13627–13637. [CrossRef]
222. González-Mancebo, D.; Becerro, A.I.; Caro, C.; Gómez-González, E.; García-Martín, M.L.; Ocaña, M. Nanoparticulated Bimodal Contrast Agent for Ultra-High-Field Magnetic Resonance Imaging and Spectral X-Ray Computed Tomography. *Inorg. Chem.* **2024**, *63*, 10648–10656. [CrossRef] [PubMed]
223. Shi, H.; Niu, M.; Tan, L.; Liu, T.; Shao, H.; Fu, C.; Ren, X.; Ma, T.; Ren, J.; Li, L.; et al. A Smart All-in-One Theranostic Platform for CT Imaging Guided Tumor Microwave Thermotherapy Based on IL@ZrO_2 Nanoparticles. *Chem. Sci.* **2015**, *6*, 5016–5026. [CrossRef]
224. Simão, T.; Chevallier, P.; Lagueux, J.; Côté, M.-F.; Rehbock, C.; Barcikowski, S.; Fortin, M.-A.; Guay, D. Laser-Synthesized Ligand-Free Au Nanoparticles for Contrast Agent Applications in Computed Tomography and Magnetic Resonance Imaging. *J. Mater. Chem. B* **2016**, *4*, 6413–6427. [CrossRef]
225. Fu, L.; Yang, S.; Jiang, S.; Zhou, X.; Sha, Z.; He, C. One-Step Synthesis of Multifunctional Nanoparticles for CT/PA Imaging Guided Breast Cancer Photothermal Therapy. *Colloids Surf. B Biointerfaces* **2021**, *201*, 111630. [CrossRef]
226. Zhang, Y.; Wen, S.; Zhao, L.; Li, D.; Liu, C.; Jiang, W.; Gao, X.; Gu, W.; Ma, N.; Zhao, J.; et al. Ultrastable Polyethyleneimine-Stabilized Gold Nanoparticles Modified with Polyethylene Glycol for Blood Pool, Lymph Node and Tumor CT Imaging. *Nanoscale* **2016**, *8*, 5567–5577. [CrossRef]
227. Ahmad, M.Y.; Liu, S.; Tegafaw, T.; Saidi, A.K.A.A.; Zhao, D.; Liu, Y.; Nam, S.-W.; Chang, Y.; Lee, G.H. Heavy Metal-Based Nanoparticles as High-Performance X-Ray Computed Tomography Contrast Agents. *Pharmaceuticals* **2023**, *16*, 1463. [CrossRef] [PubMed]
228. Barbosa, R.C.S.; Mendes, P.M. A Comprehensive Review on Photoacoustic-Based Devices for Biomedical Applications. *Sensors* **2022**, *22*, 9541. [CrossRef] [PubMed]

229. Reddy, G.R.; Bhojani, M.S.; McConville, P.; Moody, J.; Moffat, B.A.; Hall, D.E.; Kim, G.; Koo, Y.-E.L.; Woolliscroft, M.J.; Sugai, J.V.; et al. Vascular Targeted Nanoparticles for Imaging and Treatment of Brain Tumors. *Clin. Cancer Res.* **2006**, *12*, 6677–6686. [CrossRef]
230. Li, S.; Su, W.; Wu, H.; Yuan, T.; Yuan, C.; Liu, J.; Deng, G.; Gao, X.; Chen, Z.; Bao, Y.; et al. Targeted Tumour Theranostics in Mice via Carbon Quantum Dots Structurally Mimicking Large Amino Acids. *Nat. Biomed. Eng.* **2020**, *4*, 704–716. [CrossRef]
231. MacCuaig, W.M.; Jones, M.A.; Abeyakoon, O.; McNally, L.R. Development of Multispectral Optoacoustic Tomography as a Clinically Translatable Modality for Cancer Imaging. *Radiol. Imaging Cancer* **2020**, *2*, e200066. [CrossRef] [PubMed]
232. Assi, H.; Yang, C.; Shaswary, E.; Tam, M.; Tavakkoli, J.; Kolios, M.; Peyman, G.; Kumaradas, C. Real-Time Control of Nanoparticle-Mediated Thermal Therapy Using Photoacoustic Imaging. *IEEE Trans. Biomed. Eng.* **2021**, *68*, 2188–2194. [CrossRef]
233. Liu, C.; Li, C.; Jiang, S.; Zhang, C.; Tian, Y. pH-Responsive Hollow Fe–Gallic Acid Coordination Polymer for Multimodal Synergistic-Therapy and MRI of Cancer. *Nanoscale Adv.* **2021**, *4*, 173–181. [CrossRef] [PubMed]
234. Tian, C.; Zhu, L.; Lin, F.; Boyes, S.G. Poly(Acrylic Acid) Bridged Gadolinium Metal–Organic Framework–Gold Nanoparticle Composites as Contrast Agents for Computed Tomography and Magnetic Resonance Bimodal Imaging. *ACS Appl. Mater. Interfaces* **2015**, *7*, 17765–17775. [CrossRef]
235. Kircher, M.F.; de la Zerda, A.; Jokerst, J.V.; Zavaleta, C.L.; Kempen, P.J.; Mittra, E.; Pitter, K.; Huang, R.; Campos, C.; Habte, F.; et al. A Brain Tumor Molecular Imaging Strategy Using a New Triple-Modality MRI-Photoacoustic-Raman Nanoparticle. *Nat. Med.* **2012**, *18*, 829–834. [CrossRef]
236. Zhang, Z.-A.; Xin, X.; Liu, C.; Liu, Y.; Duan, H.-X.; Qi, L.; Zhang, Y.-Y.; Zhao, H.; Chen, L.-Q.; Jin, M.-J.; et al. Novel Brain-Targeted Nanomicelles for Anti-Glioma Therapy Mediated by the ApoE-Enriched Protein Corona in Vivo. *J. Nanobiotechnol.* **2021**, *19*, 453. [CrossRef]
237. Ashikbayeva, Z.; Aitkulov, A.; Jelbuldina, M.; Issatayeva, A.; Beisenova, A.; Molardi, C.; Saccomandi, P.; Blanc, W.; Inglezakis, V.J.; Tosi, D. Distributed 2D Temperature Sensing during Nanoparticles Assisted Laser Ablation by Means of High-Scattering Fiber Sensors. *Sci. Rep.* **2020**, *10*, 12593. [CrossRef]
238. Cecotka, M.; Radomski, P.; Ziółkowski, P.; Tymińska, A.; Czerwiec, K.; Zieliński, J.; Dong, Y.; Rossner, C.; Petronella, F.; Narajczyk, M.; et al. Laser Irradiation of Human Skin Tissue after Gold Nanoparticles Injection for Thermal Ablation Processes–A Combined Experimental and Numerical Approach. *Sci. Rep.* **2025**, *15*, 34422. [CrossRef] [PubMed]
239. Liu, X.; Zhou, W.; Wang, T.; Miao, S.; Lan, S.; Wei, Z.; Meng, Z.; Dai, Q.; Fan, H. Highly Localized, Efficient, and Rapid Photothermal Therapy Using Gold Nanobipyramids for Liver Cancer Cells Triggered by Femtosecond Laser. *Sci. Rep.* **2023**, *13*, 3372. [CrossRef]
240. Rocha, J.V.R.; Krause, R.F.; Ribeiro, C.E.; Oliveira, N.C.d.A.; Ribeiro de Sousa, L.; Leandro Santos, J.; Castro, S.d.M.; Valadares, M.C.; Cunha Xavier Pinto, M.; Pavam, M.V.; et al. Near Infrared Biomimetic Hybrid Magnetic Nanocarrier for MRI-Guided Thermal Therapy. *ACS Appl. Mater. Interfaces* **2024**, *17*, 13094–13110. [CrossRef]
241. Thawani, J.P.; Amirshaghaghi, A.; Yan, L.; Stein, J.M.; Liu, J.; Tsourkas, A. Photoacoustic-Guided Surgery with Indocyanine Green-Coated Superparamagnetic Iron Oxide Nanoparticle Clusters. *Small* **2017**, *13*, 1701300. [CrossRef] [PubMed]
242. Adam, A.; Mertz, D. Iron Oxide@Mesoporous Silica Core-Shell Nanoparticles as Multimodal Platforms for Magnetic Resonance Imaging, Magnetic Hyperthermia, Near-Infrared Light Photothermia, and Drug Delivery. *Nanomaterials* **2023**, *13*, 1342. [CrossRef]
243. Liu, Y.; Chang, Z.; Yuan, H.; Fales, A.M.; Vo-Dinh, T. Quintuple-Modality (SERS-MRI-CT-TPL-PTT) Plasmonic Nanoprobe for Theranostics. *Nanoscale* **2013**, *5*, 12126–12131. [CrossRef] [PubMed]
244. Farzin, A.; Etesami, S.A.; Quint, J.; Memic, A.; Tamayol, A. Magnetic Nanoparticles in Cancer Therapy and Diagnosis. *Adv. Healthc. Mater.* **2020**, *9*, 1901058. [CrossRef] [PubMed]

Disclaimer/Publisher's Note: The statements, opinions and data contained in all publications are solely those of the individual author(s) and contributor(s) and not of MDPI and/or the editor(s). MDPI and/or the editor(s) disclaim responsibility for any injury to people or property resulting from any ideas, methods, instructions or products referred to in the content.